

Ion microprobe assessment of the heterogeneity of Mg/Ca, Sr/Ca and Mn/Ca ratios in *Pecten maximus* and *Mytilus edulis* (bivalvia) shell calcite precipitated at constant temperature

P. S. Freitas^{1,2}, L. J. Clarke¹, H. Kennedy¹, and C. A. Richardson¹

¹School of Ocean Sciences, College of Natural Sciences, Bangor University, Askew Street, Menai Bridge, Isle of Anglesey, LL59 5AB, UK

²Unidade de Geologia Marinha, Laboratório Nacional de Energia e Geologia, Estrada da Portela – Zambujal, 2721-866 Alfragide, Portugal

Received: 19 December 2008 – Published in Biogeosciences Discuss.: 23 January 2009

Revised: 5 June 2009 – Accepted: 30 June 2009 – Published: 20 July 2009

Abstract. Small-scale heterogeneity of biogenic carbonate elemental composition can be a significant source of error in the accurate use of element/Ca ratios as geochemical proxies. In this study ion microprobe (SIMS) profiles showed significant small-scale variability of Mg/Ca, Sr/Ca and Mn/Ca ratios in new shell calcite of the marine bivalves *Pecten maximus* and *Mytilus edulis* that was precipitated during a constant-temperature culturing experiment. Elevated Mg/Ca, Sr/Ca and Mn/Ca ratios were found to be associated with the deposition of elaborate shell features, i.e. a shell surface stria in *P. maximus* and surface shell disturbance marks in both species, the latter a common occurrence in bivalve shells. In both species the observed small-scale elemental heterogeneity most likely was not controlled by variable transport of ions to the extra-pallial fluid, but by factors such as the influence of shell organic content and/or crystal size and orientation, the latter reflecting conditions at the shell crystal-solution interface. In the mid and innermost regions of the *P. maximus* shell the lack of significant small-scale variation of Mg/Ca ratios, which is consistent with growth at constant temperature, suggest a potential application as a palaeotemperature proxy. Cross-growth band element/Ca ratio profiles in the interior of bivalve shells may provide more promising palaeo-environmental tools than sampling from the outer region of bivalve shells.

1 Introduction

The elemental composition of marine biogenic carbonates has been thought to provide a powerful tool to obtain information on Earth's past climate and oceanographic conditions. The basis of this approach is the observed dependence of the elemental composition of marine biogenic calcite and aragonite minerals on several ambient environmental parameters, such as temperature, salinity, nutrient levels and seawater chemistry (Boyle, 1981, 1988; Lea and Boyle, 1989; Lea et al., 1989; Beck et al., 1992; Delaney et al., 1993; Nurnberg et al., 1996; Martin et al., 1999; McCulloch et al., 1999). However, biological processes and environmental parameters other than the main controlling parameters, e.g. seawater temperature for Mg/Ca ratios, also can influence the elemental composition of marine biogenic carbonates (e.g. Lorens and Bender, 1977, 1980; Delaney et al., 1985; Rosenberg et al., 1989; Rosenberg and Hughes, 1991; Klein et al., 1996a; Nurnberg et al., 1996; Lea et al., 1999; Elderfield et al., 2002; Bentov and Erez, 2005; Gillikin et al., 2005; Lorrain et al., 2005; Freitas et al., 2006). The reliable and accurate use of element/Ca ratios in marine biogenic calcite and aragonite minerals as geochemical proxies thus is dependent on quantifying the occurrence of any secondary influences on elemental incorporation.

The environmental and/or biological factor(s) that determine small-scale (<100 μm) variability in elemental composition will most likely control, to a large extent, the observed variation of element/Ca ratios in bivalve calcite at a larger scale if they are (a) major influence(s) on shell chemistry. Conventional “bulk” sampling techniques, i.e. that mill to depths of up to a few hundred microns in order to obtain



Correspondence to: P. S. Freitas
(pedro.freitas@lneg.pt)

powders for solution elemental analyses, could integrate any compositional heterogeneity to variable extents in different samples, thereby reducing spatially resolved records and introducing a significant unknown error. Thus, application of high spatial resolution analytical techniques allows a greater understanding of the implications that this compositional heterogeneity may have on the limited temperature control and large variability of Mg/Ca ratios reported for some bivalves, i.e. *Mytilus edulis* (Dodd, 1965; Klein et al., 1996b; Vander Putten et al., 2000; Freitas et al., 2008; Wanamaker et al., 2008), *Crassostrea virginica* (Surge and Lohmann, 2008) and *Pecten maximus* (Lorrain et al., 2005; Freitas et al., 2006, 2008). A greater knowledge of the extent and causes of any small-scale elemental heterogeneity also has implications for the application of Sr/Ca and Mn/Ca ratios for palaeoceanographic and palaeoenvironmental reconstructions.

Ion microprobe, or secondary ionisation mass spectrometry (SIMS), has proven extremely useful for assessing small-scale heterogeneity ($\sim 10\ \mu\text{m}$) in the distribution of thermodynamically-controlled elements, i.e. Mg in calcite and Sr in aragonite, within the shells of planktonic (Bice et al., 2005) and benthonic foraminifera (Allison and Austin, 2003), as well as corals (Allison, 1996; Cohen et al., 2001; Meibom et al., 2004; Allison et al., 2007). However, the SIMS technique has only been used previously to investigate high spatial resolution time-series variability of pollutant-type elements in bivalve shells (Jeffree et al., 1995; Siegele et al., 2001; Markich et al., 2002). Electron microprobe (Lorens and Bender, 1980; Lutz, 1981; Rosenberg and Hughes, 1991; Rosenberg et al., 2001), particle-induced X-ray emission (PIXE) (Swann et al., 1991; Siegele et al., 2001), cathodoluminescence emission (Langlet et al., 2006), proton microprobe (Coote and Trompeter, 1995), synchrotron radiation-based X-ray fluorescence (Thorn et al., 1995; Kurunczi et al., 2001) and laser ablation ICP-MS (e.g. Raith et al., 1996; Price and Pearce, 1997; Leng and Pearce, 1999; Toland et al., 2000; Vander Putten et al., 2000; Lazareth et al., 2003; Langlet et al., 2007; Barats et al., 2008, 2009) also have been used to determine spatial variability, at various different scales, in the elemental composition of bivalve shells, albeit again related to high resolution reconstructions in animals experiencing time varying environmental conditions.

For archives that retain a potential palaeotemperature proxy, such as Mg/Ca ratios, it is as critical to test the veracity of the proxy under a single constant temperature as it is to appraise the veracity of the proxy under a range of temperatures. In contrast to other biominerals produced by marine organisms, the high spatial resolution distribution of elements within bivalve shell calcite deposited at a constant temperature has not been studied in any detail. The majority of studies have focused instead on small-scale ($\sim 10\ \mu\text{m}$) temporal variability in shell chemistry, mainly on Mg/Ca ratios because of their potential application as a palaeotemperature proxy (Lorens and Bender, 1980; Rosen-

berg and Hughes, 1991; Rosenberg et al., 2001; Dauphin et al., 2003b). Other studies have focused on the small-scale variability of sulphur composition (Rosenberg et al., 2001; Dauphin et al., 2003b, 2005). By comparison, there has been limited examination of the extent and possible causes of any spatial variability in Sr/Ca or Mn/Ca ratios within marine bivalve shells (Lorens and Bender, 1980; Klein et al., 1996a; Carré et al., 2006; Barats et al., 2008), despite their potential utility as palaeoproxies. At the spatial scale of individual crystals, Dauphin et al. (2003b) observed variation in the Mg and S content of the inter- and intra-prismatic structures of the shell prismatic calcite in *Pinna nobilis* and *Pinctada margaritifera*. Significant small-scale variability of Mg/Ca and Sr/Ca ratios (from <5 to 40 mmol/mol and 0.6 to 1.6 mmol/mol, respectively) over scales of $100\ \mu\text{m}$, induced by the stress of capture and adaptation to a new laboratory environment, has been observed in new shell growth from *M. edulis* cultured in natural seawater and in semi-artificial “seawater” solutions with varying Mg/Ca and Sr/Ca ratios under controlled conditions at temperatures between 22 and 24°C (Lorens and Bender, 1980). Furthermore, Rosenberg et al. (2001) demonstrated using digital electron probe microscopy that small scale variations in Mg concentrations in *M. edulis* calcite were due to Mg being concentrated along the margins of calcite prisms, especially along the terminations of the crystals. In *M. edulis*, the Mg content of the outer calcite shell layer also was shown to be higher in regions with slow-growth, high shell curvature and with high mantle (the organ that controls calcification) activity, than in shell areas with fast shell growth, low shell curvature and low mantle activity (Rosenberg and Hughes, 1991).

In an initial preliminary assessment of the extent of any small-scale heterogeneity in Mg/Ca, Sr/Ca and Mn/Ca ratios in bivalve shell calcite, new shell material precipitated by *Pecten maximus* (king scallop) and *Mytilus edulis* (blue mussel) in a constant-temperature laboratory culturing experiment, during which other seawater parameters also were monitored, has been analysed using the ion microprobe (SIMS) technique. These two bivalve species, as well as closely related taxa, have been proposed previously as archives for palaeoceanographic studies (Krantz et al., 1988; Klein et al., 1996b; Hickson et al., 1999; Chauvaud et al., 2005; Gillikin et al., 2006; Thébaud et al., 2007; Wanamaker et al., 2007) and hence are suitable materials for such an investigation of the extent of spatial variability in bivalve shell elemental concentrations. This methodological approach is especially valid for Mg/Ca ratios in bivalve calcite, which should be invariant within the new shell growth if a simple thermodynamic influence is the predominant control on this geochemical proxy in these archival materials, and also may provide further insights into explaining the reported limited temperature control and large variability of bivalve calcite Mg/Ca ratios (Dodd, 1965; Klein et al., 1996b; Vander Putten et al., 2000; Lorrain et al., 2005; Freitas et al., 2006, 2008).

2 Materials and methods

Single specimens of *P. maximus* (shell height – the distance between the dorsal hinge and ventral margin – 34.5 mm) and *M. edulis* (shell height 29.3 mm) were selected for SIMS analysis from a group of individuals that had been cultured for 27 and 24 days, respectively, in laboratory constant-temperature aquarium (Fig. 1). The specimens used in this study were part of a larger experiment that covered a range of temperature from 10 to 20°C (Freitas et al., 2008). A temperature of 20°C was chosen for this study due to the larger shell growth at this temperature relative to 10°C or 15°C. Although 20°C is close to the high-end temperature range for these species, specimens of both species showed normal growth and no particular sign of stress. For both species studied, approximately 5–6 mm of new shell was precipitated during the total experimental period. Emergence (*M. edulis*) or handling (*P. maximus*) of each animal occurred at the beginning of the culturing period and twice more during the experiment and resulted in three “growth intervals” (denoted as T1, T2 and T3 on Figs. 2 and 3). Growth intervals are separated from one another by disturbance marks on the surface of the shell (denoted by the black vertical lines on Figs. 2 and 3), with each “growth interval” representing ca. one week’s shell growth. A combination of disturbance marks and photographs was used to identify and measure all shell growth rate (SGR) between emersions, i.e. the increase in shell height per day, and provided a time control on the new shell growth laid down throughout the experiments.

Seawater temperature in the aquarium was measured every 15 min by in-situ logger (Gemini Data Loggers TinyTag Aquatic - TGI 3080) as $20.33 \pm 0.13^\circ\text{C}$ (N=2952) and $20.21 \pm 0.13^\circ\text{C}$ (N=2304) for the duration of the two culturing periods (Fig. 1). Aquarium seawater samples for measurement of pH, element/Ca ratios and $\delta^{18}\text{O}$, were collected every second day, whereas salinity was measured on samples taken every fourth to eighth day (Fig. 1). Seawater pH measurements were taken manually with a commercial glass electrode (Mettler Toledo Inlab 412). For determination of element/Ca ratios, seawater samples were diluted 10 fold and acidified to 3% v/v with Merck Ultrapur[®] HNO₃ and measured on a Perkin Elmer Optima 3300RL ICP-AES instrument housed at the NERC ICP Facility, Royal Holloway University of London. Instrumental drift was monitored by running an independent solution, i.e. a synthetic solution of concentrations similar to seawater and that was made up from high purity single-element standards, every 10 samples. Following ICP-AES analyses, signal intensity drift was checked and corrected for to obtain the best possible analytical precision. Precision of seawater elemental analyses, expressed as relative standard deviation (RSD), was obtained from repeat measurements of the CASS-4 seawater certified reference material (Mg=42.975±0.469 μmol/ml, 1.09%RSD; Ca=8.635±0.069 μmol/ml, 0.80%RSD;

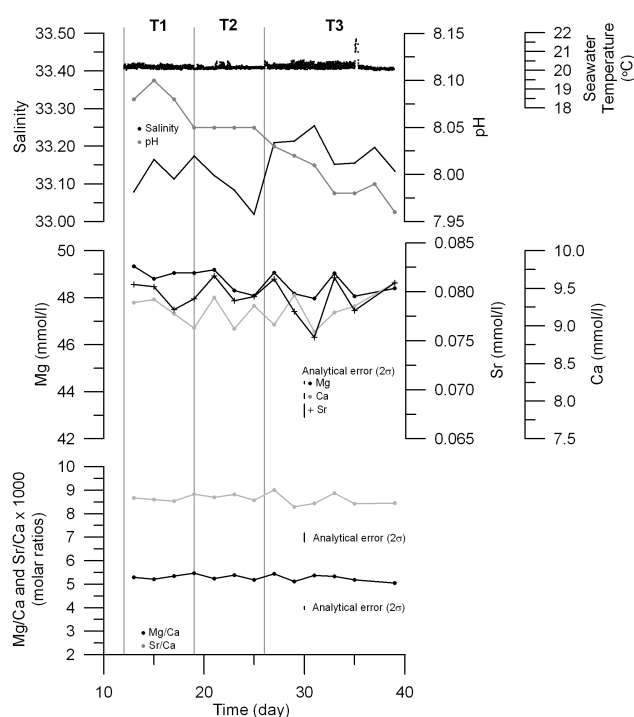


Fig. 1. Variation of seawater temperature, salinity, pH and chemistry (elemental concentrations and molar ratios) during the culturing experiment. Grey vertical lines define boundaries between different growth intervals T1, T2 and T3.

Sr=0.071±0.002 μmol/ml, 2.18%RSD;
Mg/Ca (molar)=4.977±0.079, 1.58%RSD;
Sr/Ca (molar)=0.0082±0.0002, 2.66%RSD; N=14). Aquarium seawater Mn concentrations were below the detection limits of the ICP-AES. Seawater Mg, Ca and Sr concentrations, as well as Mg/Ca and Sr/Ca molar ratios are shown in Fig. 1.

Seawater $\delta^{18}\text{O}$ and salinity samples were collected in sealed Winchester glass bottles. Seawater $\delta^{18}\text{O}$ was measured at the School of Environmental Sciences, University of East Anglia, by off-line equilibration with CO₂ and subsequent measurement of isotope ratios using a Europa-PDZ Geo 20/20 isotope-ratio mass spectrometer, with normalisation relative to a laboratory standard, North Sea Water (accepted value of +0.13‰ VSMOW). The precision of replicate $\delta^{18}\text{O}_{\text{seawater}}$ analyses is 0.05‰ (1 σ ; N=30). Seawater salinity was measured with an AutoSal 8400 Autosalinometer calibrated with International Association for Physical Sciences of the Ocean (I.A.P.S.O.) standard seawater (analytical accuracy and resolution of ±0.003 equivalent PSU). To obtain a larger temporal coverage of the salinity variation during the experiment, the following relationship, with 95% confidence intervals, between salinity and seawater $\delta^{18}\text{O}$ was obtained from paired measurements: $\text{salinity}=33.05(\pm 0.04) \times 2.53(\pm 0.46) \delta^{18}\text{O}$ ($r^2=0.96$;

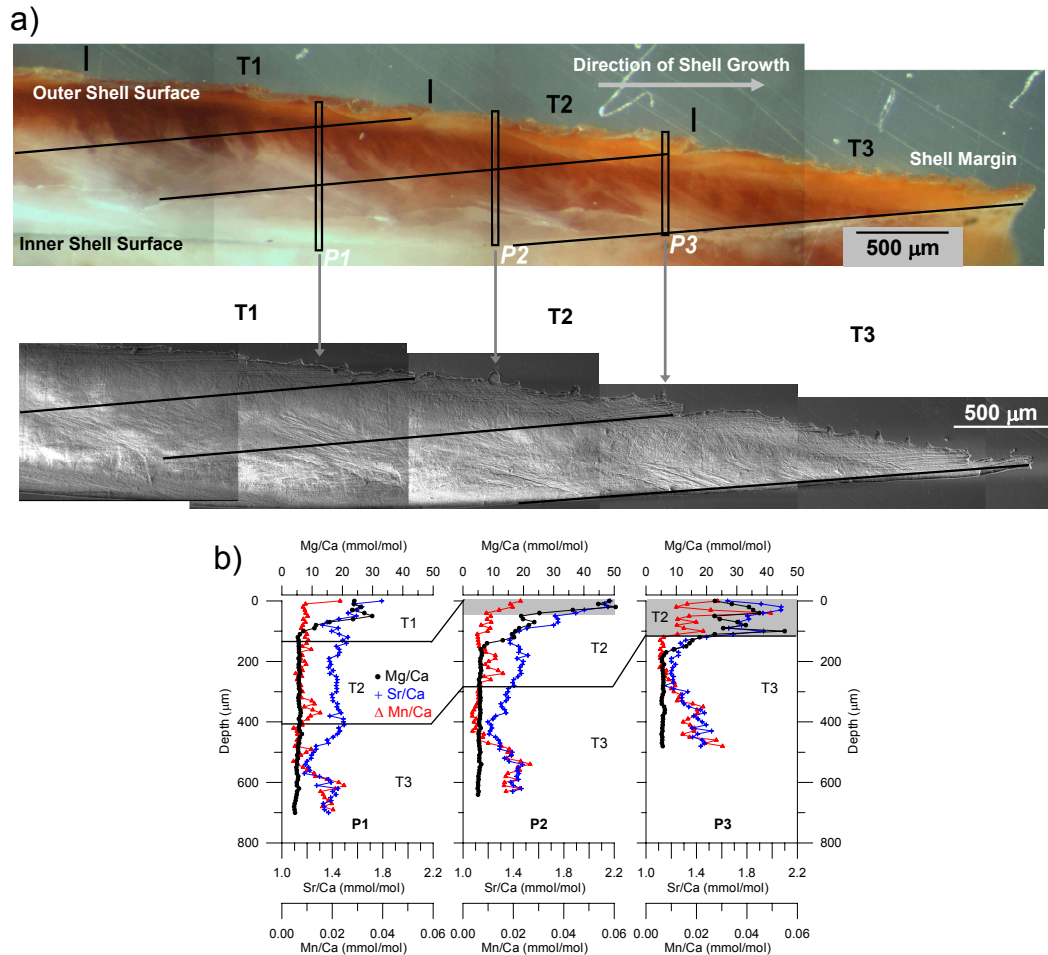


Fig. 2. (a) Light microscope photograph and SEM image of *P. maximus* with location of SIMS profiles marked (vertical black boxes) running across the shell from the outer surface to the inner surface. Grey horizontal arrow indicates the direction of shell growth. The black vertical lines mark the boundaries between three different “growth intervals”, T1, T2 and T3, and associated surface disturbance marks. The geometry of the shell has been assumed to have been the same throughout the experiment and therefore that the inner shell surface at the boundaries between the three different “growth intervals” (black diagonal lines) was parallel to the current inner shell surface. (b) SIMS Mg/Ca (black), Sr/Ca (blue) and Mn/Ca (red) ratio profiles for the *P. maximus* specimen, with depth measured from the outer shell surface towards the inner shell surface. Two profiles sampled particular features of the *P. maximus* shell (shaded areas): a shell surface stria (P2) and the region of a shell surface disturbance mark (P3). Black lines delimit the boundary between different growth intervals and were derived from the location of the black diagonal lines in Fig. 2a. Error bars are smaller than the symbols.

$p < 0.001$; $N=7$). This relationship was used to estimate salinity for those dates during the experimental period when only seawater $\delta^{18}\text{O}$ data were available ($N=16$). Salinity data are shown in Fig. 1. A full and detailed description of the culturing experiment set-up is reported elsewhere (Freitas, 2007; Freitas et al., 2008).

One shell of each bivalve species was mounted in blocks using *Robnor resins* epoxy resin (direct equivalent of araldite CY1301 and MY778) and Aradur hardener (HY951) and subsequently sectioned parallel to the main growth axis. Polished sections were digitally photographed under a light microscope and then sputter-coated with gold to inhibit build up of charge on the sample during SIMS analysis. Following

SIMS analysis the resin blocks were re-polished, etched in 0.5% acetic acid with 12.5% glutaraldehyde, sputter-coated with gold and imaged under a Cambridge-S120 scanning electron microscope to determine the shell structure of the two bivalve shells studied.

The general shell structure of *P. maximus* consists of both outer and inner irregularly oriented foliated calcite layers (Taylor et al., 1969; Carter, 1990b). The shell of *P. maximus* contains stria (growth ridges), a form of ornamentation present on the surface of the left valve. The inner layer was not observed to occur in the new growth region of the *P. maximus* specimen subjected to SIMS analyses. The general structural characteristics of *M. edulis* bivalve shells are

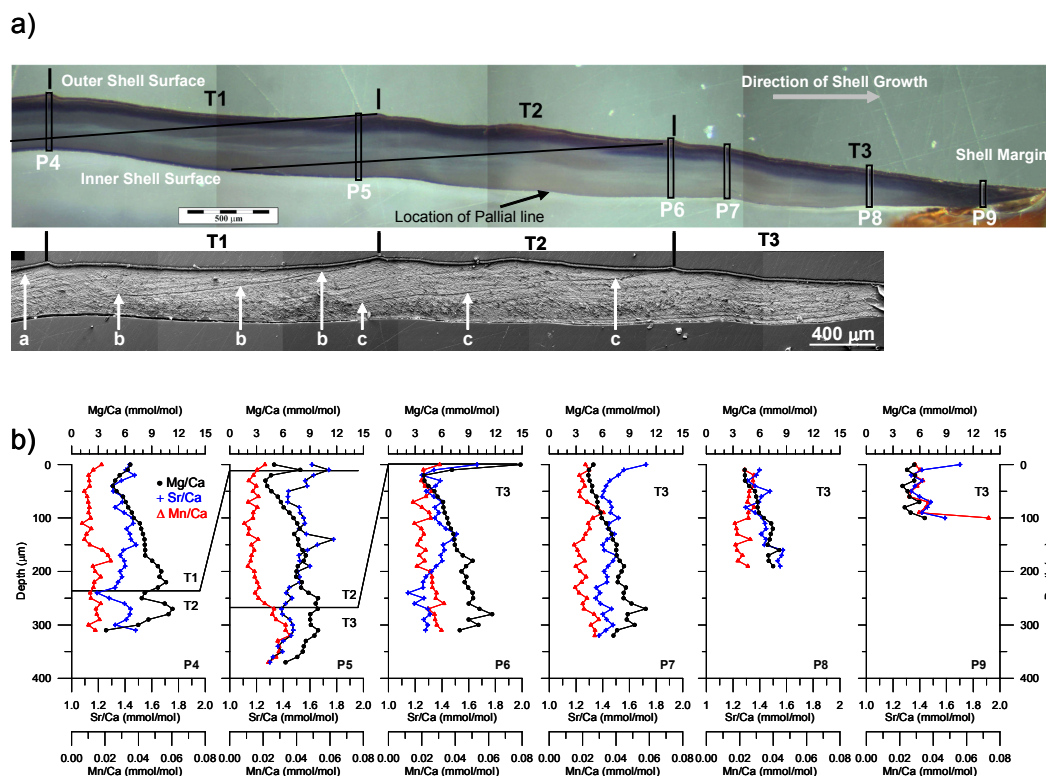


Fig. 3. (a) Light microscope photograph and SEM image of *M. edulis* with location of SIMS profiles marked (vertical black boxes) running across the shell from the outer surface to the inner surface. Grey horizontal arrow indicates the direction of shell growth. Letters a, b and c identify internal disturbance lines that are associated with the shell surface disturbance marks formed during emersion of the specimen at the beginning of the three growth intervals, T1, T2 and T3, denoted by the black vertical lines (see text and Fig. 5 for fuller discussion). In the light microscope photograph, the periostracum, which covers the outer shell surface and extends to the shell margin, is followed by a blue coloured region of ca. 100 μm thickness and then by a grey-blue coloured region down to the inner shell surface. The pallial line marks the appearance of a thin blue band on the inner shell surface and also of darker shading of the inner grey-blue shell region towards the umbo side of the pallial line, i.e. to the left in the photograph. Differences in the shell colour are not associated with differences in crystal arrangement observed in SEM images, which is similar throughout the shell. (b) SIMS Mg/Ca (black), Sr/Ca (blue) and Mn/Ca (red) ratio profiles for the *M. edulis* specimen, with depth measured from the outer shell surface towards the inner shell surface. Black lines in profiles P4 and P5 delimit the boundary between growth intervals T1–T2 and T2–T3, respectively, and were derived from the location of internal disturbance lines a, b and c in Fig. 3a. Error bars are smaller than the symbols.

two calcium carbonate layers and an outer organic layer, the periostracum, which covers the outer surface of the shell. The outer shell layer is finely prismatic calcite and the inner layer is nacreous aragonite, these separated by a thin pallial myostracum made up of irregular simple prismatic aragonite (Taylor et al., 1969; Carter, 1990a). In the new growth region of the *M. edulis* specimen subjected to SIMS analyses, the inner nacreous aragonite layer was observed on the inner shell surface between the pallial line, a mark observed on the inner shell surface that is caused by attachment of the animal's mantle organ, and the shell umbo (Fig. 3a). This layer was, however, extremely thin and if sampled by SIMS analyses was restricted to the deepest sample(s) in profiles P4 and P5. In the other profiles (P6, P7, P8 and P9) only the periostracum and outer prismatic calcite layer were sampled by SIMS analyses. Therefore, for both species, the SIMS pro-

files predominantly only spanned a single, outer, structural layer of calcite mineralogy.

Ion microprobe analyses were completed at the NERC Ion Microprobe Facility, at Edinburgh University, UK, using a Cameca ims-4f ion microprobe instrument. The optimisation of this instrument and application of the SIMS technique (Hinton, 1995) for the determination of element/Ca ratios in biogenic carbonates is described in more detail elsewhere (Allison, 1996; Allison et al., 2007). The samples were analysed using an 8–10 nA $^{16}\text{O}^-$ primary ion beam, accelerated at -10.7 keV. The sample was held at $+4.5$ keV resulting in a total impact energy of ~ 15 keV. The image setting was for 25 μm and a field aperture (number 2) was inserted to restrict the analysed area on the sample to 8–10 μm in diameter. The depth of these SIMS analyses is probably about 0.1–0.2 microns (Hinton, per-

Table 1. Summary Mg/Ca, Sr/Ca and Mn/Ca ratio data (mmol/mol) for the nine individual ion microprobe profiles (P1 to P9). 1σ is the mean standard deviation. RSD is the relative standard deviation (i.e. $1\sigma/\text{mean} \times 100$).

Mg/Ca	Min	Max	Range	Mean	N	1σ	RSD (%)
<i>P. maximus</i>							
P1	4.08	29.85	25.77	7.75	71	6.13	79
P2	4.87	50.46	45.59	10.13	65	10.41	103
P3	5.13	45.80	40.67	12.45	49	11.09	89
<i>M. edulis</i>							
P4	3.86	11.32	7.46	7.77	32	1.96	25
P5	3.99	9.91	5.92	7.54	38	1.63	22
P6	3.96	14.82	10.86	7.86	32	2.23	28
P7	4.39	10.82	6.43	7.05	33	1.67	24
P8	4.30	8.19	3.89	6.23	19	1.20	19
P9	4.05	6.56	2.51	5.10	11	0.74	15
Sr/Ca	Min	Max	Range	Mean	N	1σ	RSD (%)
<i>P. maximus</i>							
P1	1.18	1.79	0.61	1.40	71	0.11	7
P2	1.20	2.17	0.97	1.45	65	0.21	15
P3	1.14	2.07	0.93	1.45	49	0.25	17
<i>M. edulis</i>							
P4	1.19	1.48	0.29	1.39	32	0.06	5
P5	1.30	1.78	0.48	1.50	38	0.10	7
P6	1.15	1.66	0.51	1.34	32	0.10	7
P7	1.35	1.72	0.37	1.45	33	0.07	5
P8	1.29	1.57	0.28	1.43	19	0.08	6
P9	1.34	1.70	0.36	1.45	11	0.11	8
Mn/Ca	Min	Max	Range	Mean	N	1σ	RSD (%)
<i>P. maximus</i>							
P1	0.005	0.049	0.044	0.011	71	0.007	60
P2	0.004	0.051	0.047	0.012	65	0.008	65
P3	0.005	0.049	0.044	0.015	49	0.008	56
<i>M. edulis</i>							
P4	0.006	0.023	0.017	0.013	32	0.004	31
P5	0.009	0.036	0.027	0.019	38	0.007	39
P6	0.015	0.033	0.018	0.024	32	0.005	20
P7	0.015	0.032	0.017	0.022	33	0.004	20
P8	0.017	0.029	0.012	0.023	19	0.004	19
P9	0.026	0.073	0.047	0.035	11	0.013	37

sonal communication, 2007). Line profiles from the outer to inner surfaces of the two shells were undertaken in the new shell growth only using a step-size of $10\ \mu\text{m}$ resolution (Supplementary Material 1, <http://www.biogeosciences.net/6/1209/2009/bg-6-1209-2009-supplement.pdf>). The incremental growth pattern of bivalve shells is such that within an individual SIMS profile the uppermost data points are representative of shell material deposited at the shell margin at one point in time, with data points lower in that profile representing shell material precipitated subsequently, away from the shell margin at a later point in time. Therefore, the age

of the new shell material deposited during the experimental period decreases down each SIMS profile. Three profiles were completed on the *P. maximus* shell (profiles P1 to P3 in Fig. 2) and six profiles on the *M. edulis* shell (profiles P4 to P9 in Fig. 3). For both shells individual profiles traversed the full shell thickness, and in some cases also included other specific shell features, i.e. shell surface disturbance marks in both species (Figs. 2 and 3) and a shell surface stria in *P. maximus* (Fig. 2). An energy offset of $-75\ \text{eV}$ was applied to the sample and data collected with a $\pm 20\ \text{eV}$ energy window in order to minimise measurement of interferences caused by molecular ions. The ims-4f was operated in low mass resolution ($M/\Delta M=400-500$) and secondary positive ions were counted by an electron multiplier at the following masses, for counting times appropriate to the expected relative elemental concentrations: mass 22.5 (average background counts of $<1/\text{s}$; 10 s); ^{26}Mg (5 s); ^{30}Si (2 s); ^{44}Ca (2 s); ^{55}Mn (5 s); ^{88}Sr (2 s); ^{138}Ba (10 s). Mass 22.5 was selected to monitor background counts and also to allow settling of the Cameca ims-4f magnet prior to commencement of each data collection cycle. Prior to data collection, initial pre-sputtering was completed for 20 s. The ^{88}Sr signal was corrected for interference from the Ca^{2+} dimer (principally $^{48}\text{Ca}^{40}\text{Ca}^+$) using a constant Sr/Ca ratio of 0.0001, and the ^{44}Ca signal was used to identify where the individual line profiles crossed from the resin to the shell and vice versa. Silicon and barium were not above detection limits throughout the two samples. A single-point calibration was completed using the OKA carbonatite standard, including application of standardisation factors to compensate for offsets observed between SIMS and ICP-MS derived Mg/Ca and Sr/Ca ratios (Allison et al., 2007), assuming that those offsets observed for their fossil *Porites* coral aragonite are applicable to the calcite measured in this study. Nine repeat analyses of the OKA carbonatite standard were used to determine sample precisions of 2.19, 0.44 and 0.70% RSD (relative standard deviation) for the determination of Mg/Ca, Sr/Ca and Mn/Ca ratios, respectively.

3 Intra-shell spatial heterogeneity of Element/Ca ratios

Significant small-scale Mg/Ca, Sr/Ca and Mn/Ca heterogeneity was observed in both *P. maximus* and *M. edulis* shells (Figs. 2 and 3; Table 1; Supplementary Material 1, <http://www.biogeosciences.net/6/1209/2009/bg-6-1209-2009-supplement.pdf>). In *P. maximus* the range of Mg/Ca ratios (4.08 to 50.46 mmol/mol) is larger than that observed in *M. edulis* (3.86 to 14.82 mmol/mol). The range of Sr/Ca and Mn/Ca ratios was similar in the two species (Table 1), albeit with higher maximum Sr/Ca ratios in *P. maximus* (2.17 mmol/mol) than in *M. edulis* (1.78 mmol/mol) and lower maximum Mn/Ca ratios in *P. maximus* (0.051 mmol/mol) than in *M. edulis* (0.073 mmol/mol).

3.1 *Pecten maximus*

In *P. maximus* (Fig. 2b), Mg/Ca ratios in all profiles decrease from maxima in the outermost shell to a minimum value at depths of ca. 110–170 μm , below which Mg/Ca ratios were relatively invariant, both within (P1: depths of 110–700 μm , 5.46 ± 0.52 mmol/mol, N=60; P2: depths of 160–640 μm , 5.54 ± 0.32 mmol/mol, N=49; and P3: depths of 170–480 μm , 5.58 ± 0.34 mmol/mol, N=32) and between each of the three profiles, which showed no significant differences in mean Mg/Ca ratios (*t*-test, $p > 0.05$ for all comparisons). The highest Mg/Ca ratios are the highest ever reported for *P. maximus* (Lorrain et al., 2005; Freitas et al., 2008) or any other bivalve shell calcite (Lazareth et al., 2007) and were observed in regions of modified shell structures (the two shaded areas in Fig. 2b), i.e. the shell surface stria (profile P2) and disturbance growth mark (profile P3).

Shell Sr/Ca ratios were highest in the 100–120 μm of the *P. maximus* profiles proximal to the outer shell surface (1.7 to 2.2 mmol/mol), especially in the specific shell structures sampled in profiles P2 and P3 (shaded areas in Fig. 2b), i.e. the shell surface stria (up to 2.2 mmol/mol) and disturbance growth mark (up to 2.1 mmol/mol). Sr/Ca ratios then decrease to sub-surface minima (1.1 to 1.2 mmol/mol) at 200–300 μm above the inner shell surface, which in profiles P1 and P2 occur below somewhat stable intermediate ratios below the outer shell Sr/Ca maxima. Shell Sr/Ca ratios then increased from these minima to higher values towards the inner shell surface.

Shell Mn/Ca ratios were high in the ca. 100 μm proximal to the outer shell surface, particularly in the shell features sampled in profiles P2 and P3, i.e. the shell surface stria (up to 0.023 mmol/mol) and disturbance growth mark (up to 0.050 mmol/mol). Mn/Ca ratios then were lower (0.004 to 0.016 mmol/mol), but also variable, at the mid-depths within the profiles, i.e. from the ca. 100 μm proximal to the outer shell surface to 200–300 μm above the inner shell surface. Shell Mn/Ca ratios increased to higher values towards the inner shell surface (0.030 to 0.051 mmol/mol).

Taking the whole of each profile, the Sr/Ca and Mg/Ca ratios were significantly correlated (Table 2; all $p < 0.001$) in profiles P1, P2 and P3. The greatest degree of correlation was found in the 110–180 μm proximal to the outer shell surface where both Sr/Ca and Mg/Ca reach maxima (Table 2; all $p < 0.001$), and which correspond to a brighter area in the light microscope image (Fig. 2a). Between this outermost section (i.e. to depths of 110–180 μm) and the inner shell surface no significant relationship was observed between Sr/Ca and Mg/Ca ratios in any of the profiles.

Taking the whole of each profile, the Mn/Ca and Mg/Ca ratios were not significantly correlated (Table 2). However, shell Mn/Ca and Mg/Ca ratios were significantly correlated in the shell features sampled in profiles P2 and P3, i.e. the shell surface stria and disturbance growth mark (Table 2; both $p < 0.001$). Shell Mn/Ca ratios were significantly cor-

Table 2. Summary of significant ($p < 0.05$) correlations between Mg/Ca, Sr/Ca and Mn/Ca ratios for the three ion microprobe profiles (P1 to P3) in the *P. maximus* shell. “Outermost” defines a shell region between the shell surface and 110 μm , 150 μm and 200 μm depth for profiles P1, P2 and P3, respectively, where Mg/Ca ratios were highest. “Innermost” defines a shell region lower than 490 μm , 390 μm and 170 μm depth in the profiles P1, P2 and P3, respectively, where correlation between Sr/Ca and Mn/Ca ratios was highest. “All” represents the entire profiles. – indicates the absence of a significant correlation.

<i>P. maximus</i>	Mg vs Sr r^2	Mg vs Mn r^2	Mn vs Sr r^2
Outermost			
P1	0.48	0.06	0.48
P2	0.87	0.88	0.81
P3	0.77	0.49	0.45
Innermost			
P1	–	–	0.55
P2	–	–	0.82
P3	–	–	0.63
All			
P1	0.35	–	–
P2	0.83	–	0.08
P3	0.78	0.12	0.29

related to Sr/Ca ratios in profiles P1, P2 and P3 in the 110–200 μm closest to the outer shell surface and also in the 170–490 μm proximal to the inner shell surface of *P. maximus* (Table 2; all $p < 0.001$).

3.2 *Mytilus edulis*

Spatial variability of Mg/Ca, Sr/Ca and Mn/Ca ratios within the *M. edulis* shell (Fig. 3) was less systematic than in *P. maximus* (Fig. 2). Shell Mg/Ca ratios in profiles P4, P5, P6, P7 and P8 are characterised by a general increase in Mg/Ca ratios below the shell surface, which occurs in shell deposited during the three growth intervals T1, T2 and T3, to maximum values at depths of ca. 240–270 μm . Shell Mg/Ca ratios then usually decreased to lower (but not always the lowest in each profile) values at the inner shell surface. The remaining profile P9 exhibited no particular trend in Mg/Ca ratios with profile depth. Compared to Mg/Ca ratios, shell Sr/Ca and Mn/Ca ratios showed no consistent pattern with profile depth. In addition, shell Mg/Ca, Sr/Ca and Mn/Ca ratios were not significantly correlated within any of the *M. edulis* profiles ($p > 0.05$).

3.3 Relative importance of intra- and inter-profile variability in element/Ca ratios

Spatial variability of element/Ca ratios was evident both between and within each ion microprobe profile for each bivalve species (Figs. 2 and 3; Table 1). To evaluate the relative

Table 3. Mean elemental/Ca ratios (error is 1 standard error) of shell deposited during each growth interval (Fig. 3) sampled by the different SIMS profiles.

Mg/Ca	T1	T2	T3
<i>P. maximus</i>			
P1	17.11±2.45	5.77±0.04	5.15±0.11
P2	–	15.94±2.53	5.45±0.05
P3	–	32.02±2.44	6.71±0.51
<i>M. edulis</i>			
P4	7.53±0.35	8.64±0.98	–
P5	–	6.74±0.30	8.78±0.26
P6	–	–	7.86±0.40
P7	–	–	7.05±0.29
P8	–	–	6.23±0.28
P9	–	–	5.10±0.22
Sr/Ca	T1	T2	T3
<i>P. maximus</i>			
P1	1.51±0.03	1.43±0.01	1.33±0.02
P2	–	1.59±0.05	1.34±0.01
P3	–	1.86±0.05	1.32±0.02
<i>M. edulis</i>			
P4	1.38±0.01	1.40±0.03	–
P5	–	1.56±0.02	1.41±0.01
P6	–	–	1.34±0.02
P7	–	–	1.45±0.01
P8	–	–	1.43±0.02
P9	–	–	1.45±0.03
Mn/Ca	T1	T2	T3
<i>P. maximus</i>			
P1	0.010±0.001	0.009±0.001	0.013±0.002
P2	–	0.011±0.001	0.013±0.002
P3	–	0.021±0.004	0.013±0.001
<i>M. edulis</i>			
P4	0.013±0.001	0.014±0.001	–
P5	–	0.014±0.001	0.026±0.002
P6	–	–	0.024±0.001
P7	–	–	0.022±0.001
P8	–	–	0.023±0.001
P9	–	–	0.035±0.004

significance of the inter- and intra-profile heterogeneity in element/Ca ratios observed in each species, ANOVA was used to determine the percentage of the total variability that the inter- and intra-profile variation in elemental concentrations represents. Small-scale variability of element/Ca ratios in both bivalve species, with the exception of Mn/Ca ratios in *M. edulis*, was found to be dominated by intra-profile variability, i.e. between the outer and the inner shell surfaces. In both species, the majority of the variation of Mg/Ca ratios (95.6% for *P. maximus* and 83.8% for *M. edulis*) and Sr/Ca ratios (99.9% for *P. maximus* and 69.5% for *M. edulis*) occurs as intra-profile variability. A similar observation is

evident for the variability of shell Mn/Ca ratios in *P. maximus* (95.5%), whereas the relative importance of intra- and inter-profile variability of shell Mn/Ca ratios is similar in *M. edulis* (47.5 and 52.5%, respectively). In *M. edulis*, the high inter-profile variability of shell Mn/Ca ratios is evident from mean profile Mn/Ca ratios which decreased from profile P9 towards profile P4, i.e. from the shell margin towards the umbo region (Fig. 3b and Table 1).

3.4 Shell element/Ca ratio variability between growth intervals

Each individual SIMS profile sampled, at different depths, one or more growth intervals (Figs. 2 and 3) and mean element/Ca ratios can be calculated for the parts of each profile that correspond to individual growth intervals (Table 3). The comparison of mean elemental/Ca ratios for each growth interval from different profiles is hindered, however, by the influence of intra-profile variability on element/Ca ratios. This limitation is particularly true in *P. maximus* where element/Ca ratios are strongly dependent on profile depth.

Mean Mg/Ca ratios in *P. maximus* were higher in shell deposited during growth intervals T1 and T2, as sampled by SIMS profiles P1, P2 and P3 in the outermost shell, and lower in shell deposited during growth intervals T2 and T3 that were sampled by SIMS profiles P1, P2 and P3 in the innermost shell (Fig. 2 and Table 3). Mean Sr/Ca and Mn/Ca ratios in *P. maximus* were somewhat variable in shell deposited during growth intervals T1 and T2, as sampled by SIMS profiles P1, P2 and P3 in the outermost shell, but similar in shell deposited during growth interval T3, as sampled by SIMS profiles P1, P2 and P3 (Fig. 2 and Table 3).

Mean Mg/Ca and Sr/Ca ratios in *M. edulis* were similar in shell deposited during growth intervals T1, T2 and T3 as sampled by the different SIMS profiles. However, during growth interval T3, mean profile Mg/Ca ratios decreased from profile P5 towards profile P9 (Table 3), i.e. towards the shell margin. Mean profile Mn/Ca ratios in *M. edulis* were higher in SIMS profiles P5, P6, P7, P8 and P9 that sampled shell deposited during growth interval T3 and lower in profiles P4 and P5 that sampled shell deposited during growth intervals T2 and T1, respectively (Fig. 2 and Table 3).

4 Relationships between Element/Ca ratios and shell features and structure

4.1 *Pecten maximus*

SEM images (Figs. 2 and 4) illustrate that the three *P. maximus* ion microprobe profiles, situated in the new growth region of the shell, traversed only one layer of irregularly oriented foliated calcite. Nevertheless, high and variable Mg/Ca, Sr/Ca and Mn/Ca ratios are associated with some differences in the crystals arrangement, particularly within the shell surface stria (profile P2) and to a lesser extent within the

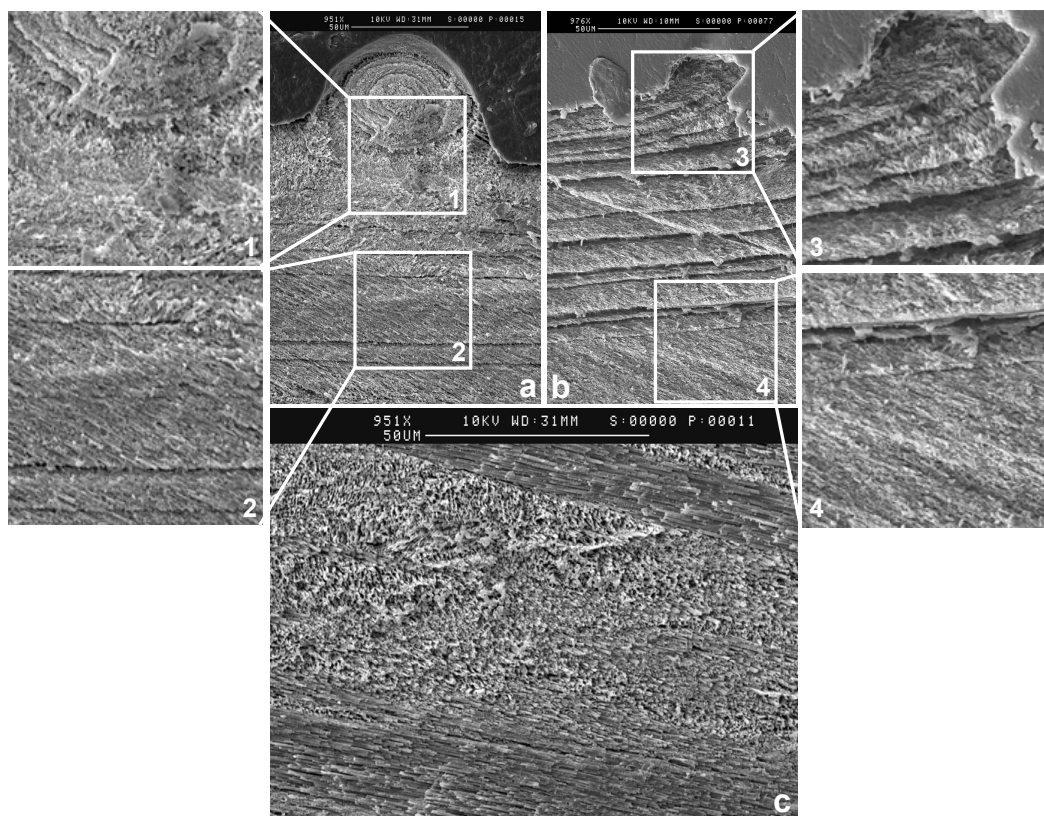


Fig. 4. Scanning electron microscope images of the *P. maximus* shell showing: (a) the shell surface stria sampled in SIMS profile P2; (b) the surface disturbance mark separating the second (T2) and third (T3) growth intervals sampled in SIMS profile P3; (c) an example of the crystal arrangement within the mid region to lowermost parts of the shell as sampled by all three SIMS profiles. Insets 1, 2, 3 and 4 are more detailed images of the contrasting crystal orientation in the shell surface stria (a) and disturbance mark (b). Images 1, 2, 3 and 4 have dimensions of $50 \times 50 \mu\text{m}$.

region of the surface disturbance mark (profile P3), which are comprised of a relatively unorganized arrangement of calcite crystals. Clearly, shell features, such as the shell surface stria and disturbance growth marks, and associated variations in crystal arrangement may well have an influence on Mg/Ca ratios in *P. maximus*, beyond any simple thermodynamic control. By comparison, Mg/Ca ratios are lower and relatively invariant in the mid region to innermost shell, whereas Sr/Ca and Mn/Ca ratios vary significantly in this region of the shell and must be controlled by some other factor other than by variable crystal arrangement. Nevertheless, the coherent variation of Sr/Ca and Mn/Ca ratios in the mid region to innermost shell for shell deposited contemporaneously during growth intervals T2 and T3, but sampled by different SIMS profiles (Fig. 2), suggests that a common process, or processes, could control both Sr and Mn incorporation in this region of the shell.

4.2 *Mytilus edulis*

All of the *M. edulis* SIMS analyses sampled the outer prismatic calcite layer (Figs. 3 and 5), and only the deepest

sample(s) closest to the inner shell surface in profiles P4 and P5 may have potentially sampled the inner nacreous aragonitic layer (see Fig. 3a and Sect. 2). Internal disturbance/growth lines are easily identifiable in the SEM images of the *M. edulis* shell (Figs. 3a and 5) and these run obliquely between the outer and inner shell surfaces. The disturbance marks on the surface of the shell (“hump-like” features where profiles P4, P5 and P6 are directly or proximally situated; Figs. 3a and 5) and their associated internal disturbance lines (the most prominent lines labelled a, b and c on Figs. 3a and 5) were formed during emersion of the animals between growth intervals, whereas the other internal growth lines formed while the animal remained immersed. It can be shown that each individual growth line, representing a common time line delimiting shell deposited contemporaneously at different locations within the shell, can be traced between SIMS profiles.

Lorenz and Bender (1980) have described previously an influence of disturbance on *M. edulis* shell Mg/Ca and Sr/Ca ratios, whereby the stress of capture and adaptation to a new laboratory environment induced the deposition of a

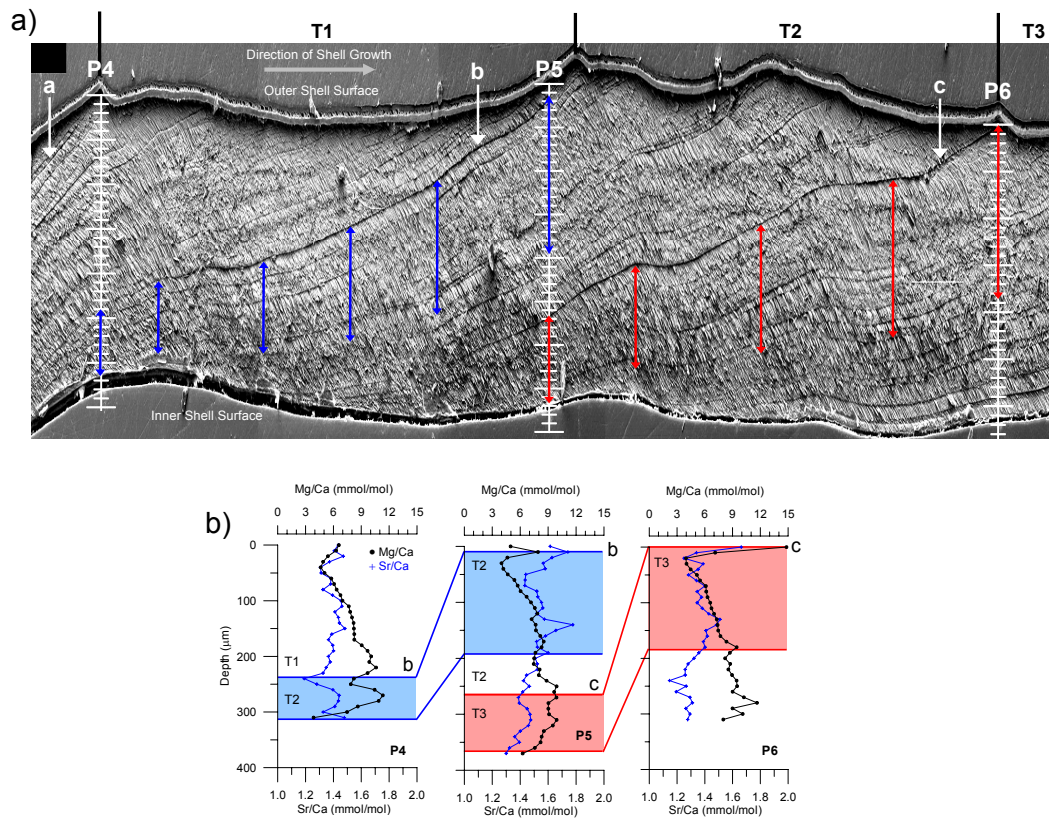


Fig. 5. (a) Scanning electron microscope images of the *M. edulis* shell with the location of each SIMS profile and individual spots indicated by the vertical line and tick marks, respectively. (b) Associated SIMS Mg/Ca and Sr/Ca ratio profiles. The “hump-like” features on the shell surface are disturbance marks deposited when the shell was emmersed at the beginning of each of the three growth intervals (T1, T2 and T3), two of which were sampled directly by SIMS profiles P4, and P6. Three internal disturbance lines (labelled a, b and c) are associated with surface disturbance marks (see also Fig. 3) and delimit the start of new shell deposited during growth intervals T1, T2 and T3, respectively. The blue and red arrows define two separate growth increments within the shell (see text for discussion), with the appropriate parts of the three SIMS profiles that correspond to these parts of the shell coloured accordingly. The shell umbo is located towards the left of the figure and the shell growing margin towards the right of the figure. (Note: for presentation purposes the image has been stretched vertically by a factor of 4). Error bars are smaller than the symbols.

shell region (termed “transition zone calcite” by those authors) with high organic matrix content and high Mg/Ca (>40 mmol/mol) and Sr/Ca (>1.4 mmol/mol) ratios. Subsequent shell growth then exhibited decreasing Mg/Ca (to <10 mmol/mol) and Sr/Ca (to <0.6 mmol/mol) ratios as the animals adapted to their new environment. However, Lorens and Bender (1980) high Mg/Ca and Sr/Ca ratio “transition zone calcite”, occurs perpendicular to the shell surface, an observation that is inconsistent with the incremental growth pattern of *M. edulis*, and suggests a strong disturbance of normal shell deposition. In this study, Mg/Ca and Sr/Ca ratios have been compared directly to SEM images of the shell’s internal growth banding, indicating a complex relationship between elemental composition and shell structure.

Given that the shell was deposited during a period of constant seawater temperature and Mg/Ca ratio, it would be expected that shell deposited between any two growth lines would have a constant Mg/Ca ratio due to contemporane-

ous precipitation, independent of the location of new mineral crystallisation within the shell. Calcite Sr/Ca and Mn/Ca ratios, on the other hand, are influenced by mineral precipitation rate in inorganic calcite, the former being positively correlated with precipitation rate (Lorens, 1981; Morse and Bender, 1990; Tesoriero and Pankow, 1996) and the latter inversely correlated to precipitation rate (Lorens, 1981; Mucci, 1988; Pingitore et al., 1988; Dromgoole and Walter, 1990). However, these observations are for inorganic calcite and thus may not be appropriate for biominerals, such as those precipitated by bivalves. If application of these observations is valid, Sr/Ca and Mn/Ca ratios are not expected to be constant throughout an individual internal shell band due to the variable mineral precipitation rates. The internal growth bands thicken towards the margin of the shell (Fig. 5), indicating that fastest shell precipitation rates occurred at the shell margin. Whereas seawater Sr/Ca ratios remained constant, due to the conservative behaviour of these

two elements, it is impossible to determine whether variable concentrations of non-conservative seawater Mn also could have contributed to the observed heterogeneity in shell Mn content since temporal changes in seawater Mn concentration were not monitored.

Interestingly, Mg/Ca ratios differ more strongly than Sr/Ca ratios depending on where shell is precipitated within two contemporaneous growth regions that were not affected by experimental emersion disturbance (Fig. 5a; regions delimited by internal disturbance lines b and c and the inner shell surface, and marked by the blue and red vertical lines). For example, shell precipitated at the shell margin during the initial part of growth increments T2 and T3 (Fig. 5b, blue and red areas at the top of profiles P5 and P6, respectively) exhibit a decrease and then a general increase in Mg/Ca and have lower mean ratios (Table 4) than shell precipitated contemporaneously in the innermost shell away from the shell margin (Fig. 5b, blue and red areas near the base of profiles P4 and P5, respectively). Furthermore, in most of the SIMS profiles Mg/Ca ratios increased with profile depth (Fig. 3 and Sect. 3.2) and such pattern is similar to that recognised by Dalbeck et al. (2006) using electron probe micro analysis, i.e. increasing Mg concentrations from the outermost shell to the base of the calcite layer. The Mg/Ca ratio variability observed within the *M. edulis* shell calcite layer in this study thus suggests that in *M. edulis* Mg/Ca ratios vary in shell precipitated contemporaneously at different locations along the inner shell surface, i.e. Mg/Ca ratios increase away from the shell margin towards the umbo. In contrast, during the initial part of growth increments T2 and T3, Sr/Ca ratios were similar (Table 4) in shell precipitated at the shell margin (Fig. 5b, blue and red areas at the top of profiles P5 and P6, respectively) and shell precipitated contemporaneously in the innermost shell away from the shell margin (Fig. 5b, blue and red areas near the base of profiles P4 and P5, respectively).

5 Potential causes of the observed small-scale Element/Ca ratio Heterogeneity within *P. maximus* and *M. edulis* Shell Calcite

The extent of the small-scale heterogeneity of element/Ca ratios differs significantly between *P. maximus* and *M. edulis*, suggesting that the processes controlling elemental incorporation into shell calcite also differ between the two bivalve species investigated in this study. For instance, *P. maximus* produces elaborate shell features, such as shell surface striae, while *M. edulis* has a smoother shell surface covered by an organic periostracum, a shell component which is absent in the former species. In addition, element/Ca ratios reached higher values in *P. maximus* than in *M. edulis*, further suggesting that elemental incorporation into shell calcite differs between these two species. Several processes can be considered as potential explanations for the differential incorporation of elements into bivalve shells and may explain the sig-

Table 4. Mean Mg/Ca and Sr/Ca ratios (N=number of samples) for *M. edulis* shell precipitated during the initial part of growth increments T2 and T3 at the outer shell surface close to the shell margin (Fig. 5, blue and red areas at the top of profiles P5 and P6, respectively) and contemporaneously in the innermost shell at the inner shell surface away from the shell margin (Fig. 5, blue and red areas near the base of profiles P4 and P5, respectively).

Region	Mg/Ca mmol/mol	Standard deviation	N	Sr/Ca mmol/mol	Standard deviation	N
Outer surface (top of profile)						
P5	8.5	1.9	18	1.49	0.08	18
P6	8.9	3.1	19	1.33	0.08	19
Inner surface (bottom of profile)						
P4	11.0	3.1	8	1.31	0.09	8
P5	11.1	1.4	11	1.34	0.06	11

nificant small-scale heterogeneity of Mg, Sr and Mn contents in *P. maximus* and *M. edulis* shell calcite that has been observed in the present study. Of all the elements investigated in this study, Mg in the outermost parts of the *P. maximus* shell provides the strongest indication for the likely presence of control(s) other than temperature on the elemental composition of bivalve calcite.

5.1 Environmental variables: seawater salinity, pH, Mg/Ca and Sr/Ca ratios, Mg and Sr concentrations

Deposition of new shell material in *P. maximus* and *M. edulis* during the laboratory-culturing experiment occurred at constant temperature and constant seawater Mg/Ca and Sr/Ca ratios (Fig. 1). However, other environmental parameters that are known to influence the elemental composition of biogenic carbonates, such as salinity and pH (e.g. for foraminifera; Nurnberg et al., 1996; Lea et al., 1999), were not constant for the duration of the experiment (Fig. 1). Nevertheless, the range of salinity (33.02 to 33.32) values and seawater Mg, Ca and Sr concentrations (and Mg/Ca and Sr/Ca molar ratios), were small during the culturing experiment (Fig. 1), and can not be associated with the variation of shell Mg/Ca Sr/Ca and Mn/Ca ratios observed in the SIMS profiles of *P. maximus* and *M. edulis* (Figs. 2 and 3). If the effect of pH on Mg/Ca ratios in bivalve calcite is similar to foraminifera calcite (Lea et al., 1999), then the 0.14 unit decrease in pH (7.96 to 8.10) values observed during this culturing experiment (Fig. 1) could explain an increase of 8.4% in Mg/Ca ratios. However, Mg/Ca ratios in *P. maximus* did not, however, increase as pH decreased (Figs. 1 and 2) and in *M. edulis* Mg/Ca ratios increased with profile depth by more than 100% (Fig. 3), even during growth interval T2 when pH was stable (Fig. 1). Any effect of pH on *P. maximus* and *M. edulis* Mg/Ca ratios is thus non-existent or fairly small. In contrast, an increase in seawater Mn concentration (not

Table 5. Shell growth rates ($\mu\text{m day}^{-1}$) during the culturing experiment for *P. maximus* and *M. edulis* specimens sampled by SIMS.

Species	Growth Interval	Shell Growth Rate
<i>P. maximus</i>	1	289
	2	210
	3	171
<i>M. edulis</i>	1	259
	2	234
	3	200

measured) during the culturing experiment could potentially explain the observed increase in mean profile Mn/Ca ratios observed in SIMS profiles that sampled *M. edulis* shell deposited from growth interval T1 to T3 (Table 1), but such a response would appear to be restricted to *M. edulis* since a similar pattern was not observed in the *P. maximus* shell Mn/Ca data.

5.2 Shell growth and mineral precipitation rates

No data on the metabolic activity and food uptake of the animals were collected during the experimental period. However, shell growth rate (SGR) was measured and should reflect changes in the physiological condition, food uptake and metabolic activity of the animals during the experiment, i.e. assuming that an increase in food uptake or metabolic activity of the animals will correspond in an increase in SGR. For both the *P. maximus* and *M. edulis* specimens, at the whole shell level, SGR decreased from growth interval T1 to T3 (Table 5) and, from the comparison to mean profile Mg/Ca, Sr/Ca and Mn/Ca ratios for each growth interval sampled by different SIMS profiles (Table 3), SGR did not influence the variation of Mg/Ca, Sr/Ca and Mn/Ca observed in the SIMS profiles of *P. maximus* and *M. edulis* (Figs. 2 and 3).

In calcite, Mg incorporation is not thought to be influenced by mineral precipitation rate, both in synthetic (e.g. Morse and Bender, 1990) and in bivalve calcite (Lorens and Bender, 1980). In inorganic synthetic calcite, which may not fully represent the biomineral precipitation of bivalve shells, increasing precipitation rate has been shown to cause an increase in Sr/Ca ratios and a reduction in Mn/Ca ratios in calcite (Lorens, 1981; Pingitore et al., 1988; Dromgoole and Walter, 1990; Morse and Bender, 1990). In addition, in *P. maximus* and *M. edulis* a strong kinetic control of Sr/Ca ratios has been reported previously (Lorrain et al., 2005; Freitas et al., 2006).

In the *M. edulis* shell the individual internal growth bands, defined by two growth lines representing contemporaneous periods of shell deposition, thicken towards the margin of the shell (Fig. 5). This observation indicates variable mineral precipitation rates with the highest shell precipitation rates occurring at the shell margin. If Sr/Ca and Mn/Ca ratios in

M. edulis were controlled by mineral precipitation rate, Sr/Ca ratios should be higher and Mn/Ca ratios lower in the shell deposited at the shell margin compared to shell deposited away from the shell margin. Such variation of Sr/Ca and Mn/Ca ratios was not, however, observed in any of the individual SIMS profiles, albeit such a pattern can be identified in one of two growth bands sampled at different locations within the shell in profiles P4, P5 and P6 (Fig. 5). Mean Sr/Ca ratios were higher in shell deposited closer to the shell margin than in shell deposited away from the shell margin (Table 4 and Fig. 5b; blue areas shaded on the top of profile P5 and at the bottom of profile P4, respectively). Nevertheless, from this single observation mineral precipitation rate cannot be considered to exert a significant general influence on the incorporation of Sr and Mn in the shell calcite of *M. edulis*.

A similar comparison cannot be made for *P. maximus* due to the lack of visible internal growth lines. It can be seen, however, that Sr and Mn positively co-vary in the innermost shell regions (Fig. 2 and Table 2) and thus Sr and Mn incorporation in *P. maximus* calcite could well be controlled by a common process(es) other than precipitation rate.

5.3 Composition of the extra-pallial fluid (EPF), the precipitating solution in bivalves

The elemental composition of the solution from which calcification occurs is known to have a strong influence on the incorporation of Mg, Sr and Mn in calcite (Mucci and Morse, 1983; Pingitore and Eastman, 1986; Dromgoole and Walter, 1990).

In both *P. maximus* and *M. edulis*, Mg/Ca, Sr/Ca and Mn/Ca ratios varied significantly in shell deposited from the same marginal EPF at the same time, but at different locations on the inner shell surface. The observed variation of element/Ca ratios with profile depth, particularly for Mg/Ca ratios in *P. maximus*, suggests that such variability mainly reflects differences in location of shell formation rather than differences in the time of shell formation. Transport to the EPF likely is not a major control on the observed heterogeneity of shell elemental composition, unless variation of ion transport along the mantle could lead to elemental concentration gradients within the EPF. Other smaller-scale mechanism(s) thus must control incorporation of elements in the shell, e.g. processes that act at the shell crystal-solution interface. Furthermore, the mantle epithelium and the shell surface are in close proximity, being either separated by a small distance and may be in contact with each other, and the transfer of ions and organic molecules may occur virtually by direct contact (Simkiss and Wilbur, 1989; Addadi et al., 2006). This process thus could provide the potential for small-scale variations in the chemical and physical conditions at different precipitation sites on the growing shell surface.

5.4 Elemental composition of shell calcite

The Mg content of calcite is known to influence the incorporation of other elements during calcite precipitation, whereby substitution for Ca^{2+} by Mg^{2+} distorts the crystal lattice and favours the incorporation of other elements, namely ones with large ionic radii, such as Sr^{2+} and Mn^{2+} (Mucci and Morse, 1983; Ohde and Kitano, 1984; Morse and Bender, 1990). In *P. maximus*, significant positive correlations were observed between Mg/Ca and both Sr/Ca and Mn/Ca ratios in the 100–200 μm proximal to the outer shell surface, particularly in the shell surface stria and disturbance mark. Therefore, shell Mg content could influence Sr and, to a lesser extent, Mn incorporation in the outermost part of the shell of this species (Table 2), where Mg/Ca ratios are highest (10–50 mmol/mol, Fig. 2). Such a lattice distortion control is not, however, evident in the mid region and innermost part of the *P. maximus* shell. In this same part of the shell Mg does not correlate with Sr or Mn, but Sr and Mn are significantly correlated to each other (Table 2), suggesting that a common process, or processes, could control both Sr and Mn incorporation. In *M. edulis*, Mg/Ca ratios were not significantly correlated to Sr/Ca and Mn/Ca, and thus shell Mg content does not appear to have influenced Sr and Mn incorporation in the calcite shell component of this species.

5.5 Calcite crystal orientation and size

Sector zoning is a phenomenon recognised in both synthetic and natural calcite minerals, whereby differences in elemental composition occur both within a particular crystal sector type (intra-sectoral) and between crystallographically non-equivalent coeval growth sectors (inter-sectoral) in any one crystal (Reeder and Grams, 1987; Reeder and Paquette, 1989; Paquette and Reeder, 1990, 1995). It should be noted, however, that such phenomena might not be applicable to biogenic calcites. Elemental zoning patterns reflect non-equilibrium elemental incorporation due to differences in the intrinsic characteristics of crystal surfaces and their underlying structure, the specific nature of co-ordination environments and the crystal-growth mechanism, but not due to crystal growth rates (Reeder and Grams, 1987; Reeder and Paquette, 1989; Paquette and Reeder, 1990, 1995).

Unlike laser-ablation or powder milling sampling, SIMS instrumentation samples only about 0.1–0.2 microns of the polished shell section (Hinton, personal communication, 2007). Therefore, if those calcite crystals comprising the sectioned bivalve shells were orientated along different growth axes within different parts of shells then the observed variability in the SIMS element/Ca ratio data could be explained by the SIMS sampling of different crystal faces with variable elemental composition due to inter-sectoral zoning, as described above.

Dalbeck et al. (2006) used Electron Backscatter Diffraction (EBSD) and electron probe microanalysis (EPMA) to

investigate the relative crystallographic orientations of crystals and chemistry, respectively, of *M. edulis* calcite and aragonite layers. For the entire calcite layer of this species, with the exception of the outermost 40 μm , Dalbeck et al. (2006) demonstrated uniformity of the axes of the individual calcite crystals, which differ in orientation to one another by less than 15°. Calcite crystals in the outermost 40 μm are morphologically more varied than the remainder of the calcite layer, with a progressive refinement in the orientation of the planes of adjacent crystals during shell growth toward the inner shell surface (Dalbeck et al., 2006). Consequently, SIMS sampling of different crystal faces cannot be used as an explanation for the observed variability of Mg/Ca, Sr/Ca and Mn/Ca ratios within the majority of *M. edulis* calcite sampled herein (Fig. 3), but cannot be discounted in the outermost 40 μm of the *M. edulis* shell. A similar conclusion was reached by Dalbeck et al. (2006) in terms of the compositional variability evident in their EPMA elemental dataset. In addition, Dalbeck et al. (2006) have suggested that the smaller size of the calcite crystals in the outermost part of the *M. edulis* shell may allow a greater adsorption of cations due to a greater surface area to volume ratio. Rosenberg et al. (2001) also observed in *M. edulis* that Mg is concentrated along the margins of calcite prisms, especially along the terminations of the crystals, which correspond to shell disturbance growth marks (Dalbeck et al., 2006), i.e. to changes in the normal shell deposition and orientation of the shell calcite crystals.

For *P. maximus*, Checa et al. (2007) have shown that the foliated calcite layer of this bivalve species is made up of highly organised folia that display a coherent crystallographic pattern, i.e. a sheet texture; several co-existing sets of folia run in different directions (see also Fig. 4c). As with *M. edulis*, the uniformity of crystal orientation within *P. maximus* folia means that SIMS sampling of different crystal faces cannot be invoked as an explanation for variable Mg/Ca, Sr/Ca and Mn/Ca within a folia. Furthermore, the relatively uniform element/Ca ratios in the interior of the *P. maximus* shell discard SIMS sampling of co-existing sets of folia running in different directions, and thus potentially of different crystal faces, as a source of variability in Mg/Ca, Sr/Ca and Mn/Ca ratios. In the shell surface stria (profile P2) and surface disturbance mark (profile P3) crystals were more randomly orientated than in the interior of the shell (Fig. 4), an observation also reported for the related species *Pecten diegensis* (Clark, 1974). As such, it is impossible to discount the possibility that more random crystal orientations contribute to the high Mg/Ca, Sr/Ca and Mn/Ca ratios observed in these regions as the result of SIMS sampling of different crystal faces with variable elemental composition. Support for such reasoning is found in the strong correlations observed between the Mg/Ca, Sr/Ca and Mn/Ca ratios measured in this study within the shell surface stria and disturbance mark and the evidence for positive correlations between Mg, Mn and Sr concentrations in different crystal

growth sectors, i.e. elevated within the same sector relative to another sector (Reeder and Grams, 1987; Reeder and Paquette, 1989). Without detailed EBSD studies, however, further speculation regarding the effect of crystal orientation on the Mg/Ca, Sr/Ca and Mn/Ca ratios of bivalve shell calcite is unwarranted.

5.6 Role of the shell organic matrix

Biogenic minerals are composed of both inorganic and organic fractions, the latter controlling crystal nucleation and growth (e.g., Mann, 2001; Weiner and Dove, 2003; Addadi et al., 2006). Within and between shells the organic matrix varies both in concentration and composition (e.g. Dauphin, 2003; Dauphin et al., 2003a, 2005) and may, therefore, influence elemental incorporation and distribution within marine bivalve shells, by distorting the calcite crystal lattice (Pokroy et al., 2006) or by itself incorporating and/or adsorbing elements.

The role of the organic matrix on elemental incorporation in biogenic carbonates is, however, far from clear and may likely vary between specific taxa. For instance, removal of the organic component of the aragonitic shell of the estuarine bivalve *Corbula amurensis* results in a lowering of shell Mg and Mn concentrations, but not of Sr content (Takesue et al., 2008). In the shell calcite of the gastropod *Concholepas concholepas* lower Mg content occurs in areas with higher organic content (Lazareth et al., 2007). In two species of brachiopods, *Terbratulina retusa* and *Notosaria nigricans*, Mg has been shown not to be hosted by organic components (Cusack et al., 2008b).

Sulphur has been proposed to represent the shell organic matrix, either as sulphated polysaccharides or S-rich aminoacids, in biogenic carbonates such as bivalves (Lorens and Bender, 1980; Rosenberg et al., 2001; Dauphin et al., 2003a, 2003b, 2005), gastropods (Lazareth et al., 2007), brachiopods (Cusack et al., 2008a) and corals (Cuif and Dauphin, 2005). Observations that the distribution of Mg correlates with S variability has led to the suggestion that a proportion of the measured Mg content in biogenic calcites is non-lattice bound, being associated with the shell organic matrix (Lorens and Bender, 1980; Rosenberg and Hughes, 1991; Rosenberg et al., 2001; England et al., 2007). For instance, in *M. edulis*, shell regions with high curvature are organic-rich and have high Mg and S content in contrast to shell regions with low curvature that are mineral-rich and have low Mg and S content (Rosenberg et al., 1989; Rosenberg and Hughes, 1991; Rosenberg et al., 2001). However, sulphur can also occur in the calcite structure as sulphate that substitutes for carbonate groups (Kontrec et al., 2004), and thus the use of S as a tracer for the organic matrix in biogenic carbonates is not straightforward. For instance, in the calcite shells of the bivalves *P. nobilis* and *P. margaritifera* no correlation was observed between Mg and S (Dauphin et al., 2003b), whereas in the shell calcite of the gastropod *C. con-*

cholepas Mg and S were observed to be inversely correlated (Lazareth et al., 2007).

The deposition of complex features, such as the surface ridge and disturbance growth marks, involves a marked disruption of shell deposition in *P. maximus*, with changes in the orientation of the shell surface and also of calcite crystal orientation (Figs. 2 and 4). Lorens and Bender (1980) observed that high S/Ca and Mg/Ca ratios were both found in *M. edulis* shell regions deposited under stress conditions and suggested that *M. edulis* compensates for increased Mg levels in the extra-pallial fluid (EPF), which inhibits calcite nucleation and crystal growth (Berner, 1975), by secreting additional S-bearing organic matrix to aid mineralization. Furthermore, it has been proposed that *M. edulis* uses Mg and S (as a component of the organic matrix) to control shell crystal elongation and hence shell form (Rosenberg et al., 2001). Therefore, considering the observations of Lorens and Bender (1980), Rosenberg et al. (1989, 2001) and Rosenberg and Hughes (1991), it is plausible that deposition of the surface ridge and disturbance growth marks in *P. maximus* involves an increase in the organic matrix relative to the remainder of the shell and that such an increase is associated with higher Mg contents, although not necessarily bound to the organic matrix. In *M. edulis*, the disruption of shell deposition associated with disturbance growth marks appears to be of smaller intensity and is not associated with higher Mg/Ca ratios (Figs. 3 and 5). However, in the mid region of the *M. edulis* shell Mg/Ca ratios increased with profile depth (i.e. from the outer towards the inner shell surface) in all but one of the SIMS profiles (Fig. 3). It is thus plausible that such an increase in Mg/Ca ratios, from the outer towards the inner shell surfaces corresponds to an increase in the organic matrix content. This suggestion would imply that organic matrix content varies with the location of shell precipitation at the inner shell surface, i.e. organic matrix content increases from the shell margin towards the umbo.

Variations in both the amount and type of the shell organic matrix remain plausible causes of the SIMS element/Ca ratio heterogeneity observed in this study, especially with regards to the shell surface stria in *P. maximus* and the disturbance growth marks evident in *P. maximus* and *M. edulis*.

6 Small-scale element heterogeneity and implications for the use of geochemical proxies in bivalves

It is clear from the ion microprobe elemental data collected in this study that, for both bivalve species investigated herein, highly variable Mg/Ca, Sr/Ca and Mn/Ca ratios can occur within one structural layer of shell calcite precipitated at a single and constant seawater temperature and via deposition from the same marginal extra-pallial fluid (EPF), albeit a variably non-isolated EPF in *P. maximus*. Such significant small-scale heterogeneity of the Mg, Sr and Mn content in the shells of *M. edulis* and *P. maximus* has profound

implications for the application of these geochemical proxies in bivalve calcite. First, the deposition of elaborate shell features and surface disturbance growth marks, the latter ubiquitous features of shells of many bivalve shells, is associated with highly variable element/Ca ratios. Second, factors/processes that may influence elemental incorporation into bivalve calcite potentially do not just operate at the scale of whole shells, or even within a single shell structural layer, but can vary at tens of microns scale. Third, users of large-scale “bulk” shell sampling methods, and even micro-sampling methods, such as electron or ion microprobe or laser ablation sampling, need to consider carefully which section, or sections, of the shell are sampled, otherwise they risk obtaining a large variability in element/Ca ratio measurements that does not relate to any change in environmental conditions. Finally, Mg, Sr and Mn incorporation into bivalve calcite most likely is under the control of multiple factors and the relative influence of any one factor most likely varies with time and with the location of the shell deposition.

In particular, significant small-scale heterogeneity (i.e. tens of microns) in bivalve shell Mg/Ca ratios is potentially a significant source of error when attempting to use Mg/Ca ratios of these biogenic calcites in palaeotemperature reconstructions. For instance, *M. edulis* and *P. maximus* specimens grown in the same experiment as the ones analysed by SIMS in the present study, but sampled by surface milling, displayed a large variability (up to ca. 6 mmol/mol and up to ca. 16 mmol/mol, respectively) in Mg/Ca ratios at constant temperature and a weak correlation between shell Mg/Ca ratios and seawater temperature ($r^2=0.37$, $p<0.001$ and $r^2=0.21$, $p<0.001$, respectively) was observed over a range from 10 to 20°C (Freitas et al., 2008). It is clear from the ion microprobe data obtained in this study that small-scale variability in the Mg content is one possible reason why such a weak relationship was observed between shell Mg/Ca ratios and seawater temperature in *P. maximus* (Lorrain et al., 2005; Freitas et al., 2006, 2008). The inclusion of variable amounts of material from parts of the shell structure with different Mg/Ca ratios, such as the shell surface striae and/or surface disturbance marks, provides a possible explanation for the lack of temperature control and for the large variability of Mg/Ca ratios observed in *P. maximus* (Lorrain et al., 2005; Freitas et al., 2006, 2008). In another field-based culturing experimental study, the unexpected increase in Mg/Ca ratios of *P. maximus* specimens grown at low winter temperatures (Freitas et al., 2006) could be explained by a higher number of shell surface striae (ca. 12 striae/mm) being milled and included in each “winter” powder sample, compared to Mg/Ca ratios in spring and summer samples with a lower number of shell surface striae (ca. 4–6 striae/mm), which exhibited a more robust relationship to water temperatures.

In *M. edulis* there is some evidence that Mg/Ca ratios vary significantly depending on whether shell deposition occurs at the shell margin or on the inner shell surface. The observation that *M. edulis* shell Mg/Ca ratios are influenced by

disturbance marks formed during emersion could be particularly significant since in a natural inter-tidal environment the twice daily emersion-immersion cycles control the internal and surficial growth banding of *M. edulis* shells. Furthermore, disturbance marks are ubiquitous in *M. edulis* shells, as well as in other bivalve species, and can reflect interruption of shell deposition during periods of environmental and/or physiological stress (Richardson, 2001). Such observations further question the validity, and indicate the difficulty, of using Mg/Ca ratios in *M. edulis* as a palaeotemperature proxy, irrespective of a previous study that demonstrated a Mg/Ca ratio-temperature relationship in the related species *M. trossulus* (Klein et al., 1996b).

7 The potential of Mg/Ca ratios in the innermost shell region of *P. maximus* as a palaeotemperature proxy

In contrast to the high and variable Mg/Ca ratios in the outermost shell, the relatively invariant Mg/Ca ratios in the mid to innermost shell of *P. maximus* suggest a region of shell deposition where temperature was the main control on Mg incorporation with a strong potential to use measurements of the Mg/Ca ratio in this part of the shells of this bivalve species as a palaeotemperature proxy. Such a hypothesis is strengthened by the evidence that the Mg/Ca ratios were relatively invariant both within and between each of the three profiles in the mid region and lowermost shell sampled, even though deposition occurred at different times and locations along the inner shell surface (Fig. 2).

8 Summary

In the present study, significant heterogeneity in Mg/Ca, Sr/Ca and Mn/Ca ratios within the new growth of shells of *P. maximus* and *M. edulis* deposited at a constant temperature of 20°C has been determined using SIMS. Differences in the relative contribution of specific shell features, i.e. the number and size of shell surface striae (in *P. maximus*) and surface disturbance growth marks (in both species) milled, as well as the depth of milling through regions of shell with variable Mg/Ca, Sr/Ca and Mn/Ca ratios, likely explains some of the variability in element/Ca ratios observed previously for *M. edulis* and *P. maximus* shells. Most importantly, the observed variation in Mg/Ca ratios, as well as in Sr/Ca and Mn/Ca ratios, cannot be attributed to particular structural shell layers that are recognised for *P. maximus* or *M. edulis* shells, since only one structural layer was sampled by the SIMS analyses. In *P. maximus*, Mg appears to strongly influence the incorporation of Sr and Mn in the uppermost shell, while in the innermost shell of this species Sr and Mn co-vary, an observation that suggests incorporation of these two elements may be controlled by a common process or processes.

The present study clearly confirms that processes that control shell structure and features can exert a strong influence on the elemental composition of bivalve shell calcite, even in shell deposited from the same solution. Therefore, it is evident that disruption of “normal” shell deposition significantly perturbs the elemental composition of shell calcite in these species. The common presence of shell features and growth marks in bivalve shells thus further questions the use of Mg/Ca, Sr/Ca and Mn/Ca from bivalve calcite as valid geochemical proxies. In *P. maximus*, however, the invariant Mg/Ca ratios of the mid and internal regions of the shell were shown to be predominantly under a thermodynamic control, and therefore the potential to use measurements of the Mg/Ca ratio in this part of the shells of this animal as a palaeotemperature proxy is confirmed.

Acknowledgements. The authors thank Berwyn Roberts and Gwyn Hughes for their ever-present technical support in relation to the maintenance of the laboratory aquaria and supply of algal cultures during the laboratory culturing experiment, John Rowlands for technical support during use of the scanning electron microscope and David Oakes from Ramsay Sound Shellfish Ltd. for supplying the scallop specimens. Access to the U.K. Natural Environment Research Council Ion Microprobe Facility at Edinburgh University and the assistance of Richard Hinton and John Craven is acknowledged gratefully. We thank Renee Takesue, Claire Lazareth, Vincent Salters and an anonymous reviewer for their constructive comments that substantially improved this manuscript. This research was partially funded by Fundação para a Ciência e Tecnologia (FCT), Portugal, through a scholarship to Pedro Freitas, Contract No. SFRH/BD/10370/2002.

Edited by: D. Hammarlund

References

- Addadi, L., Joester, D., Nudelman, F., and Weiner, S.: Mollusk shell formation: A source of new concepts for understanding biomineralization processes, *Chem. Eur. J.*, 12, 980–987, 2006.
- Allison, N.: Comparative determination of trace and minor elements in coral aragonite by ion microprobe analysis, with preliminary results from Phuket, southern Thailand, *Geochim. Cosmochim. Ac.*, 60, 3457–3470, 1996.
- Allison, N. and Austin, W.: The potential of ion microprobe analysis in detecting geochemical variations across individual foraminifera tests, *Geochem. Geophys. Geosy.*, 4, 8403, doi:8410.1029/2002GC000430, 2003.
- Allison, N., Finch, A. A., Webster, J. M., and Clague, D. A.: Palaeoenvironmental records from fossil corals: The effects of submarine diagenesis on temperature and climate estimates, *Geochim. Cosmochim. Ac.*, 71, 4693–4703, 2007.
- Barats, A., Amouroux, D., Pécheyran, C., Chauvaud, L., and Donard, O. F. X.: High-Frequency Archives of Manganese Inputs To Coastal Waters (Bay of Seine, France) Resolved by the LA-ICP-MS Analysis of Calcitic Growth Layers along Scallop Shells (*Pecten maximus*), *Environ. Sci. Technol.*, 42, 86–92, 2008.
- Barats, A., Amouroux, D., Chauvaud, L., Pécheyran, C., Lorrain, A., Thebault, H., Church, T., and Donard, O.: High frequency Barium profiles in shells of the Great Scallop *Pecten maximus*: a methodical long-term and multi-site survey in Western Europe, *Biogeosciences*, 6, 157–170, 2009, <http://www.biogeosciences.net/6/157/2009/>.
- Beck, J., Edwards, R., Ito, E., Taylor, F., Recy, J., Rougerie, F., Joannot, P., and Henin, C.: Sea surface temperature from skeletal Sr/Ca ratios, *Science*, 257, 644–647, 1992.
- Bentov, S. and Erez, J.: Novel observations on biomineralization processes in foraminifera and implications for Mg/Ca ratio in the shells, *Geology*, 33, 841–844, 2005.
- Berner, R.: The role of magnesium on the crystal growth of calcite and aragonite in seawater, *Geochim. Cosmochim. Ac.*, 39, 489–504, 1975.
- Bice, K., Layne, G., and Dahl, K.: Application of secondary ion mass spectrometry to the determination of Mg/Ca in rare, delicate, or altered planktonic foraminifera: Examples from the Holocene, Paleogene, and Cretaceous, *Geochem. Geophys. Geosy.*, 6, Q12P07, doi:10.1029/2005GC000974, 2005.
- Boyle, E.: Cadmium, zinc, copper and barium in foraminifera tests, *Earth Planet. Sc. Lett.*, 53, 11–35, 1981.
- Boyle, E.: Cadmium: Chemical tracer of deepwater paleoceanography, *Paleoceanography*, 471–489, 1988.
- Carré, M., Bentaleb, I., Bruguier, O., Ordinola, E., Barret, N., and Fontugne, M.: Calcification rate influence on trace element concentrations in aragonitic bivalve shells: Evidences and mechanisms, *Geochim. Cosmochim. Ac.*, 70, 4906–4920, 2006.
- Carter, J.: Shell microstructural data for the Bivalvia. Part VI. Order Mytiloidea, in: *Skeletal Biomineralization: Patterns, Processes and Evolutionary Trends*, edited by: Carter, J., 1, Van Nostrand Reinhold, New York, 390–406, 1990a.
- Carter, J.: Shell microstructural data for the Bivalvia. Part V. Order Pectinoidea, in: *Skeletal Biomineralization: Patterns, Processes and Evolutionary Trends*, edited by: Carter, J., 1, Van Nostrand Reinhold, New York, 363–389, 1990b.
- Chauvaud, L., Lorrain, A., Dunbar, R., Paulet, Y. M., Thouzeau, G., Jean, F., Guarini, J., and Mucciarone, D.: Shell of the Great Scallop *Pecten maximus* as a high-frequency archive of paleoenvironmental changes, *Geochem. Geophys. Geosy.*, 6, Q08001, doi:08010.1029/02004GC000890, 2005.
- Checa, A., Esteban-Delgado, F., and Rodríguez-Navarro, A.: Crystallographic structure of the foliated calcite of bivalves, *J. Struct. Biol.*, 157, 393–402, 2007.
- Clark II, G. R.: Calcification on an unstable substrate: marginal growth in the mollusc *Pecten diegensis*, *Science*, 183, 968–970, 1974.
- Cohen, A., Layne, G., Hart, S., and Lobel, P.: Kinetic control of skeletal Sr/Ca in a symbiotic coral: Implications for the paleotemperature proxy, *Paleoceanography*, 16, 20–26, 2001.
- Coote, G. E. and Trompeter, W. J.: Proton microprobe studies of fluorine distributions in mollusc shells, *Nucl. Instrum. Meth. B*, 104, 333–338, 1995.
- Cuif, J. P. and Dauphin, Y.: The Environment Recording Unit in coral skeletons: a synthesis of structural and chemical evidences for a biochemically driven, stepping-growth process in fibres, *Biogeosciences*, 2, 61–73, 2005, <http://www.biogeosciences.net/2/61/2005/>.

- Cusack, M., Dauphin, Y., Cuif, J.-P., Salomé, M., Freer, A., and Yin, H.: Micro-XANES mapping of sulphur and its association with magnesium and phosphorus in the shell of the brachiopod, *Terebratulina retusa*, *Chem. Geol.*, 253, 172–179, 2008a.
- Cusack, M., Pérez-Huerta, A., Janousch, M., and Finch, A. A.: Magnesium in the lattice of calcite-shelled brachiopods, *Chem. Geol.*, 257, 59–64, 2008b.
- Dalbeck, P., England, J., Cusack, M., Lee, M., and Fallick, A.: Crystallography and chemistry of the calcium carbonate polymorph switch in *M. edulis* shells, *Eur. J. Mineral.*, 18, 601–609, 2006.
- Dauphin, Y.: Soluble organic matrices of the calcitic prismatic shell layers of two pteriomorphid bivalves - *Pinna nobilis* and *Pinctada margaritifera*, *J. Biol. Chem.*, 278, 15 168–15 177, 2003.
- Dauphin, Y., Cuif, J. P., Doucet, J., Salome, M., Susini, J., and Williams, C. T.: In situ chemical speciation of sulfur in calcitic biominerals and the simple prism concept, *J. Struct. Biol.*, 142, 272–280, 2003a.
- Dauphin, Y., Susini, J., Williams, C. T., Cuif, J. P., Doucet, J., and Salomé, M.: In situ mapping of growth lines in the calcitic prismatic layers of mollusc shells using X-ray absorption near-edge structure (XANES) spectroscopy at the sulphur K-edge, *Mar. Biol.*, 142, 299–304, 2003b.
- Dauphin, Y., Cuif, J. P., Salome, C., and Susini, J.: Speciation and distribution of sulfur in a mollusk shell as revealed by in situ maps using X-ray absorption near-edge structure (XANES) spectroscopy at the sulphur K-edge, *Am. Mineral.*, 90, 1748–1758, 2005.
- Delaney, M. L., Be, A. W. H., and Boyle, E. A.: Li, Sr, Mg, and Na in foraminiferal calcite shells from laboratory culture, sediment traps, and sediment cores, *Geochim. Cosmochim. Ac.*, 49, 1327–1341, 1985.
- Delaney, M. L., Linn, L. J., and Druffel, E. R. M.: Seasonal cycles of manganese and cadmium in coral from the Galapagos Islands, *Geochim. Cosmochim. Ac.*, 57, 347–354, 1993.
- Dodd, J.: Environmental control of strontium and magnesium in *Mytilus*, *Geochim. Cosmochim. Ac.*, 29, 385–398, 1965.
- Dromgoole, E. and Walter, L.: Iron and manganese incorporation into calcite: effects of growth kinetics, temperature and solution chemistry, *Chem. Geol.*, 81, 311–336, 1990.
- Elderfield, H., Vautravers, M., and Cooper, M.: The relationship between shell size and Mg/Ca, Sr/Ca, $\delta^{18}\text{O}$, and $\delta^{13}\text{C}$ of species of planktonic foraminifera, *Geochem. Geophys. Geosy.*, 3, 1052, doi:10.1029/2001GC000194, 2002.
- England, J., Cusack, M., and Lee, M.: Magnesium and sulphur in the calcite shells of two brachiopods, *Terebratulina retusa* and *Novocrania anomala*, *Lethaia*, 40, 2–10, 2007.
- Freitas, P., Clarke, L., Kennedy, H., Richardson, C. A., and Abrantes, F.: Environmental and biological controls on elemental (Mg/Ca, Sr/Ca and Mn/Ca) ratios in shells of the king scallop *Pecten maximus*, *Geochim. Cosmochim. Ac.*, 70, 5119–5133, 2006.
- Freitas, P.: Environmental and Biological Controls of Mg/Ca, Sr/Ca and Mn/Ca Ratios in the Shells of the Bivalves *Mytilus edulis* and *Pecten maximus*: Implications for Palaeoenvironmental Reconstructions, PhD, School of Ocean Sciences, Bangor University, Bangor, U.K., 242 pp., 2007.
- Freitas, P. S., Clarke, L. J., Kennedy, H. A., and Richardson, C. A.: Inter- and intra-specimen variability masks reliable temperature control on shell Mg/Ca ratios in laboratory- and field-cultured *Mytilus edulis* and *Pecten maximus* (bivalvia), *Biogeosciences*, 5, 1245–1258, 2008, <http://www.biogeosciences.net/5/1245/2008/>.
- Gillikin, D., Lorrain, A., Navez, J., Taylor, J., Andre, L., Keppens, E., Baeyens, W., and Dehairs, F.: Strong biological controls on Sr/Ca ratios in aragonitic marine bivalve shells, *Geochem. Geophys. Geosy.*, 6, Q05009, doi:05010.01029/02004GC000874, 2005.
- Gillikin, D., Dehairs, F., Lorrain, A., Steenmans, D., Baeyens, W., and Andre, L.: Barium uptake into the shell of the common mussel (*Mytilus edulis*) and the potential for paleo-chemistry reconstruction, *Geochim. Cosmochim. Ac.*, 70, 395–407, 2006.
- Hickson, J. A., Johnson, A. L. A., Heaton, T. H. E., and Balson, P. S.: The shell of the Queen Scallop *Aequipecten opercularis* (L.) as a promising tool for palaeoenvironmental reconstruction: evidence and reasons for equilibrium stable-isotope incorporation, *Palaeogeogr. Palaeoclimatol. Palaeoecol.*, 154, 325–337, 1999.
- Hinton, R.: Ion microprobe analysis in geology, in: *Microprobe Techniques in the Earth Sciences*, edited by: Potts, P. J., Bowles, J. F. W., Reed, S. J. B., and Cave, M. R., Chapman and Hall, New York, 235–290, 1995.
- Jeffree, R., Markich, S., Lefebvre, F., Thellier, M., and Ripoll, C.: Shell microlaminations of the fresh-water bivalve *Hyridella depressa* as an archival monitor of manganese concentration - Experimental investigation by depth profiling using secondary-ion mass-spectrometry (SIMS), *Experientia*, 51, 838–848, 1995.
- Klein, R., Lohmann, K., and Thayer, C.: Sr/Ca and $^{13}\text{C}/^{12}\text{C}$ ratios in skeletal calcite of *Mytilus trossulus*: Covariation with metabolic rate, salinity and carbon isotopic composition of seawater, *Geochim. Cosmochim. Ac.*, 60, 4207–4221, 1996a.
- Klein, R., Lohmann, K., and Thayer, C.: Bivalve skeletons record sea-surface temperatures and $\delta^{18}\text{O}$ via Mg/Ca and $^{18}\text{O}/^{16}\text{O}$ ratios, *Geology*, 24, 415–418, 1996b.
- Kontrec, J., Kralj, D., Brecevic, L., Falini, G., Fermani, S., Noethig-Laslo, V., and Miroslavljevic, K.: Incorporation of inorganic anions in calcite, *Eur. J. Inorg. Chem.*, 2004(23), 4579–4585, 2004.
- Krantz, D., Kronick, A., and Williams, D.: A model for interpreting continental shelf hydrographic processes from the stable isotope and cadmium: calcium profiles of scallop shells, *Palaeogeogr. Palaeoclimatol.*, 64, 123–140, 1988.
- Kurunczi, S., Torok, S., and Chevallier, P.: A micro-XRF study of the element distribution on the growth front of mussel shell (Species of *Unio crassus Retzius*), *Mikrochim. Acta*, 137, 41–48, 2001.
- Langlet, D., Alunno-Bruscia, M., Rafelis, M., Renard, M., Roux, M., Schein, E., and Buestel, D.: Experimental and natural cathodoluminescence in the shell of *Crassostrea gigas* from Thau lagoon (France): ecological and environmental implications, *Mar. Ecol.-Prog. Ser.*, 317, 143–156, 2006.
- Langlet, D., Alleman, L., Plisnier, P.-D., Hughes, H., and André, L.: Manganese content records seasonal upwelling in Lake Tanganyika, *Biogeosciences*, 4, 195–203, 2007, <http://www.biogeosciences.net/4/195/2007/>.
- Lazareth, C. E., Vander Putten, E., Andre, L., and Dehairs, F.: High-resolution trace element profiles in shells of the mangrove bivalve *Isognomon ephippium*: a record of environmental spatio-temporal variations?, *Estuar. Coast. Shelf S.*, 57, 1103–1114, 2003.

- Lazareth, C. E., Guzman, N., Poitrasson, F., Candaudap, F., and Ortlieb, L.: Nyctemeral variations of magnesium intake in the calcitic layer of a Chilean mollusk shell (*Concholepas concholepas*, Gastropoda), *Geochim. Cosmochim. Ac.*, 71, 5369–5383, 2007.
- Lea, D. and Boyle, E.: Barium content of benthic foraminifera controlled by bottom-water composition, *Nature*, 338, 751–753, 1989.
- Lea, D. W., Shen, G., and Boyle, E.: Coralline barium records temporal variability in equatorial upwelling, *Nature*, 340, 373–376, 1989.
- Lea, D. W., Mashiotta, T., and Spero, H.: Controls on magnesium and strontium uptake in planktonic foraminifera determined by live culturing, *Geochim. Cosmochim. Ac.*, 63, 2369–2379, 1999.
- Leng, M. and Pearce, N.: Seasonal variation of trace element and isotopic composition in the shell of a coastal mollusk, *Mactra isabelleana*, *J. Shellfish Res.*, 18, 569–574, 1999.
- Lorens, R. and Bender, M.: Physiological exclusion of magnesium from *Mytilus edulis* calcite, *Nature*, 269, 793–794, 1977.
- Lorens, R. and Bender, M.: The impact of solution chemistry on *Mytilus edulis* calcite and aragonite, *Geochim. Cosmochim. Ac.*, 44, 1265–1278, 1980.
- Lorens, R.: Sr, Cd, Mn and Co distribution coefficients in calcite as a function of calcite precipitation rate, *Geochim. Cosmochim. Ac.*, 45, 553–561, 1981.
- Lorrain, A., Gillikin, D., Paulet, Y. M., Chavaud, L., Lemerrier, A., Navez, J., and Andre, L.: Strong kinetic effects on Sr/Ca ratios in the calcitic bivalve *Pecten maximus*, *Geology*, 33, 965–968, 2005.
- Lutz, R.: Electron probe analysis of strontium in mussel (*Bivalvia*: *Mytilidae*) shells: Feasibility of estimating water temperature, *Hydrobiologia*, 83, 377–382, 1981.
- Mann, S.: *Biom mineralization: Principles and Concepts in Bioinorganic materials Chemistry*, Oxford University Press, New York, 198 pp., 2001.
- Markich, S., Jeffree, R., and Burke, P.: Freshwater bivalve shells as archival indicators of metal pollution from a copper-uranium mine in tropical northern Australia, *Environ. Sci. Technol.*, 36, 821–832, 2002.
- Martin, P., Lea, D., Mashiotta, T., Papenfuss, T., and Sarthein, M.: Variation of foraminiferal Sr/Ca over Quaternary glacial-interglacial cycles: Evidence for changes in mean ocean Sr/Ca?, *Geochem. Geophys. Geos.*, 1, 1004, doi:10.1029/1999GC000006, 1999.
- McCulloch, M., Tudhope, A., Esat, T., Mortimer, G., Chappell, J., Pilans, B., Chivas, A., and Omuta, A.: Coral record of equatorial sea-surface temperatures during the penultimate deglaciation at Huon Peninsula, *Science*, 283, 202–204, 1999.
- Meibom, A., Cuif, J. P., Hillion, F. O., Constantz, B., Juillet-Leclerc, A., Dauphin, Y., Watanabe, T., and Dunbar, R.: Distribution of magnesium in coral skeleton, *Geophys. Res. Lett.*, 31, L23306, doi:23310.21029/22004GL021313, 2004.
- Morse, J. and Bender, M.: Partition coefficients in calcite: Examination of factors influencing the validity of experimental results and their application to natural systems, *Chem. Geol.*, 82, 265–277, 1990.
- Mucci, A. and Morse, J.: The incorporation of Mg^{2+} and Sr^{2+} into calcite overgrowths: Influences of growth rate and solution composition, *Geochim. Cosmochim. Ac.*, 47, 217–233, 1983.
- Mucci, A.: Manganese uptake during calcite precipitation from seawater: Conditions leading to the formation of pseudokutnahorite, *Geochim. Cosmochim. Ac.*, 52, 1859–1868, 1988.
- Nurnberg, D., Bijma, J., and Hemleben, C.: Assessing the reliability of magnesium in foraminiferal calcite as a proxy for water mass temperatures, *Geochim. Cosmochim. Ac.*, 60, 803–814, 1996.
- Ohde, S. and Kitano, Y.: Coprecipitation of strontium with marine Ca-Mg carbonates, *Geochem. J.*, 18, 143–146, 1984.
- Paquette, J. and Reeder, R.: New type of compositional zoning in calcite: Insights into crystal-growth mechanisms, *Geology*, 18, 1244–1247, 1990.
- Paquette, J. and Reeder, R.: Relationship between surface structure, growth mechanism and trace element incorporation in calcite, *Geochim. Cosmochim. Ac.*, 54, 395–402, 1995.
- Pingitore, J., Nicholas E., Eastman, M., Sandidge, M., Oden, K., and Freiha, B.: The coprecipitation of manganese (II) with calcite: an experimental study, *Mar. Chem.*, 25, 107–120, 1988.
- Pingitore, N., and Eastman, M.: The coprecipitation of Sr^{2+} with calcite at 25°C and 1 atm, *Geochim. Cosmochim. Ac.*, 50, 2195–2203, 1986.
- Pokroy, B., Fitch, A. N., Marin, F., Kapon, M., Adir, N., and Zolotoyabko, E.: Anisotropic lattice distortions in biogenic calcite induced by intra-crystalline organic molecules, *J. Struct. Biol.*, 155, 96–103, 2006.
- Price, G., and Pearce, N.: Biomonitoring of pollution by *Cerastoderma edule* from the British Isles: a laser ablation ICP-MS study, *Mar. Pollut. Bull.*, 34, 1025–1031, 1997.
- Raith, A., Perkins, W., Pearce, N., and Jeffries, T.: Environmental monitoring on shellfish using UV laser ablation ICP-MS, *Fresenius J. Anal. Chem.*, 355, 789–792, 1996.
- Reeder, R. and Paquette, J.: Sector zoning in natural and synthetic calcites, *Sediment. Geol.*, 65, 239–247, 1989.
- Reeder, R. J. and Grams, J. C.: Sector zoning in calcite cement crystals: Implications for trace element distributions in carbonates, *Geochim. Cosmochim. Ac.*, 51, 187–194, 1987.
- Richardson, C.: Molluscs as archives of environmental change, *Oceanogr. Mar. Biol.*, 39, 103–164, 2001.
- Rosenberg, G., Hughes, W., and Tkachuck, R.: Shell form and metabolic gradients in the mantle of *Mytilus edulis*, *Lethaia*, 22, 343–344, 1989.
- Rosenberg, G., and Hughes, W.: A metabolic model for the determination of shell composition in the bivalve mollusc, *Mytilus edulis*, *Lethaia*, 24, 83–96, 1991.
- Rosenberg, G. D., Hughes, W. W., Parker, D. L., and Ray, B. D.: The geometry of bivalve shell chemistry and mantle metabolism, *Am. Malacol. Bull.*, 16, 251–261, 2001.
- Siegele, R., Orlic, I., Cohen, D., Markich, S., and Jeffree, R.: Manganese profiles in freshwater mussel shells, *Nucl. Instrum. Meth. B*, 181, 593–597, 2001.
- Simkiss, K. and Wilbur, K.: *Biom mineralization: Cell biology and mineral deposition*, Academic Press, San Diego, 337 pp., 1989.
- Surge, D. and Lohmann, K.: Evaluating Mg/Ca ratios as a temperature proxy in the estuarine oyster, *Crassostrea virginica*, *J. Geophys. Res.*, 113, G02001, doi:02010.01029/02007JG000623, 2008.
- Swann, C. P., Hansen, K. M., Price, K., and Lutz, R.: Application of PIXE in the study of shellfish, *Nucl. Instrum. Meth. B*, 56–57, 683–686, 1991.

- Takesue, R. K., Bacon, C. R., and Thompson, J. K.: Influences of organic matter and calcification rate on trace elements in aragonitic estuarine bivalve shells, *Geochim. Cosmochim. Ac.*, 72, 5431–5445, 2008.
- Taylor, J. D., Kennedy, W. J., and Hall, A.: The shell structure and mineralogy of the Bivalvia: Introduction, Nuculacea-Trigonacea, *Bulletin British Museum (Nat. Hist.) Zoology*, 3, 1–125, 1969.
- Tesoriero, A., and Pankow, J.: Solid solution partitioning of Sr^{2+} , Ba^{2+} and Cd^{2+} to calcite, *Geochim. Cosmochim. Ac.*, 60, 1053–1063, 1996.
- Thébault, J., Chauvaud, L., Clavier, J., Guarini, J., Dunbar, R. B., Fichez, R., Mucciarone, D. A., and Morize, E.: Reconstruction of seasonal temperature variability in the tropical Pacific Ocean from the shell of the scallop, *Comptopallium radula*, *Geochim. Cosmochim. Ac.*, 71, 918–928, 2007.
- Thorn, K., Cerrato, R., and Rivers, M.: Elemental distributions in marine bivalves shells as measured by synchrotron X-ray fluorescence, *Biol. Bull.*, 188, 57–67, 1995.
- Toland, H., Perkins, B., Pearce, N., Keenan, F., and Leng, M.: A study of sclerochronology by laser ablation ICP-MS, *J. Anal. Atom. Spectrom.*, 15, 1143–1148, 2000.
- Vander Putten, E., Dehairs, F., Keppens, E., and Baeyens, W.: High resolution distribution of trace elements in the calcite shell layer of modern *Mytilus edulis*: Environmental and biological controls, *Geochim. Cosmochim. Ac.*, 64, 997–1011, 2000.
- Wanamaker, A., Kreutz, K., Borns, H., Introne, D., Feindel, S., Funder, S., Rawson, P., and Barber, B.: Experimental determination of salinity, temperature, growth, and metabolic effects on shell isotope chemistry of *Mytilus edulis* collected from Maine and Greenland, *Paleoceanography*, 22, PA2217, doi:2210.1029/2006PA001352, 2007.
- Wanamaker, A., Kreutz, K., Wilson, T., Borns Jr, H., Introne, D., and Feindel, S.: Experimentally determined Mg/Ca and Sr/Ca ratios in juvenile bivalve calcite for *Mytilus edulis*: Implications for paleotemperature reconstructions, *Geo-Mar. Lett.*, 28(5–6), 359–368, doi:10.1007/s00367-00008-00112-00368, 2008.
- Weiner, S. and Dove, P.: Overview of biomineralization processes and the problem of the vital effects, in: *Biomaterialization*, edited by: Dove, P., De Yoreo, J., and Weiner, S., *Reviews in Mineralogy and Geochemistry*, 54, Mineralogical Society of America, Washington, USA, 1–29, 2003.